

2017

Analysis of Newtonian Viscous Flows Through Tubes of Arbitrary Varying Cross Sections

Edgardo Daniel Fernandez
Lehigh University

Follow this and additional works at: <http://preserve.lehigh.edu/etd>



Part of the [Mechanical Engineering Commons](#)

Recommended Citation

Fernandez, Edgardo Daniel, "Analysis of Newtonian Viscous Flows Through Tubes of Arbitrary Varying Cross Sections" (2017). *Theses and Dissertations*. 2589.

<http://preserve.lehigh.edu/etd/2589>

This Thesis is brought to you for free and open access by Lehigh Preserve. It has been accepted for inclusion in Theses and Dissertations by an authorized administrator of Lehigh Preserve. For more information, please contact preserve@lehigh.edu.

Analysis of Newtonian Viscous Flows
Through Tubes of Arbitrary Varying
Cross Sections

by

Edgardo Daniel Fernández Díaz

April 19 , 2017

Certificate of Approval

This thesis is accepted and approved in partial fulfillment of the requirements for the Master of Science degree in Mechanical Engineering.

Date

Thesis Advisor

Chairperson of Department

Acknowledgement

All my gratitude and respect to professor Jacob Kazakia for his support as advisor in this work and through the entire master of science distance learning program.

To Andrea and Emma for all their patience and support.

Contents

1	Viscous Flows Through Bounded Regions	1
1.1	Viscous Flow Basics	1
1.2	Mathematical Description of Newtonian Fluids Motion	2
1.3	Laminar Viscous Flow Through Tubes of Elliptic Cross Section	6
2	Numerical Solution for Laminar Viscous Flow Through Tubes of Varying Cross Section	14
2.1	Numerical Solution for Laminar Viscous Flow Through Tubes of Arbitrary Constant Cross Section	15
2.2	Numerical Solutions by Finite Element Method	16
2.3	Flow Through Arbitrary Varying Cross Section - Numerical Solutions .	21
2.4	Alternative Numerical Perturbation	22
3	Laminar Flow Through Arbitrary Varying Cross Section	29
3.1	Perturbation Approximation	29
3.2	Solution by Perturbation Approximation	34
4	Implementation of Numerical Solutions on Practical Cases	40
4.1	Design of Numerical Experiments Procedure	41
4.2	Results of Numerical Experiments	43

4.2.1	Influence of Aspect Ratio on Pressure Distribution	43
4.2.2	Uncertainty Analysis for Ellipse	47
5	Conclusions	53

List of Figures

1.1	Schematic Diagram of Viscous Experiment	3
1.2	Elliptical cross section mapped onto cylindrical space	8
1.3	Analytic solutions for some cross section. Ref.[4]	10
2.1	Unit velocity distribution for different cross sections and maximum unit value where u obtained by numerical analysis. $\epsilon = b^2/(a^2 + b^2)$	19
4.1	Elliptical section with eccentricity b/a	42
4.2	Pressure Distribution ($m=2/200$)	43
4.3	Pressure Distribution ($m=2/200$)	44
4.4	Pressure Distribution: Flow rate q_1 , ellipse ($b/a=1/2, m=1/200$)	45
4.5	Pressure Distribution: Flow rate q_{13} , ellipse ($b/a=1/2, m=1/200$)	45
4.6	Pressure Distribution: Flow rate q_1 , ellipse ($b/a=1/2, m=2/200$)	46
4.7	Pressure Distribution: Flow rate q_{13} , ellipse ($b/a=1/2, m=2/200$)	46
4.8	Pressure Relative Error ($b/a=1/2, m=1/200$)	47
4.9	Pressure Relative Error ($b/a=1/2, m=2/200$)	48
4.10	Pressure Relative Error Flow Rate q_1 ($b/a=1/2, m=1/200$)	48
4.11	Pressure Relative Error Flow Rate q_3 ($b/a=1/2, m=1/200$)	49
4.12	Pressure Relative Error Flow Rate q_5 ($b/a=1/2, m=1/200$)	49

4.13 Pressure Relative Error Flow Rate q_7 ($b/a=1/2, m=1/200$)	50
4.14 Pressure Relative Error Flow Rate q_9 ($b/a=1/2, m=1/200$)	50
4.15 Pressure Distribution Rectangle ($b/a=1/2, m=2/200$)	51
4.16 Relative Error Rectangle Flow Rate q_{13} ($b/a=1/2, m=1/200$)	51

List of Tables

2.1	Analytic and numerical results for some known cross sections	20
4.1	Flow properties and geometry description	42

Abstract

Newtonian viscous flows under laminar regime across tubes of arbitrary varying cross sections were analyzed. The simple form of this problem for constant circular cross section is a well known result from the early years of Fluid Mechanics.[1] Nowadays, many modern applications such as nanotubes manufacturing, MEMS, Biomechanics and medical procedures, require to determine pressure losses for Newtonian and non Newtonian fluids in tubes with varying geometries. These applications have renewed the interest in this classical problem and the search for accurate solutions based on numerical, analytic and experimental methods.[2]

In the present work, several methods were explored as means to determine pressure gradients for arbitrary shapes and varying cross sections. In all cases, non dimensional forms of momentum equation were employed. The motivation to work with non dimensional expressions was clearly justified by the fact that in laminar regime, velocity distributions are basically the same for any cross section as long as its shape remains constant. Thus, once the numerical solution is found for a typical section, solution for any other section can be obtained by a re scaling process of by an appropriate characteristic length. This approach enabled to determine not only pressure gradients, but also Fanning's friction factor for any shape.

Lubrication approximation and perturbation of axial convective acceleration term

were first addressed. Non dimensional numerical solutions by finite element method were implemented in a computer code developed for this purpose as part of the work. Results were compared to analytic solutions [2,3,4] for elliptical cross sections exhibiting good correlation for small aspect ratios (*characteristic length / axial length*) along the tube. Furthermore, an *alternative regular perturbation* approach applied to viscous and axial convective acceleration was tested. A computer code was also developed to implement finite element solution for this approach. Results were in good correlation with analytic results based on lubrication and perturbations methods previously detailed. Finally, a different approach identified as *convective acceleration correction* was defined. In this case, the effect that transverse acceleration components have on axial velocity throughout the tube were considered. Once again, a non dimensional form of the momentum equation was developed and solved by means of finite element procedure. In all cases, convective acceleration correction exhibited less deviation in pressure gradient estimation than any other method however of which, further tests must be conducted and compared to physical experimental data in future research. Detailed analysis of uncertainties for all methods were developed for two elliptical cross sections with different aspect ratios. CFD solutions obtained from commercial software were accepted as experimental values for comparison purposes.

Chapter 1

Viscous Flows Through Bounded

Regions

1.1 Viscous Flow Basics

Fluids are materials that experience continuous deformations under the action of shear forces. Despite its complexity, fluids motion is the result of this deformation process over time. Depending on its molecular structure, fluids will exhibit some kind of resistance to deformation that eventually, will take them to rest if the action of applied external forces ceases. This behavior is explained by the presence of internal forces exerted by molecules (*collisions, electric forces*) . The macroscopic manifestation of such molecular activity determines an inherent physical property of fluids known as *Dynamic Viscosity* (μ).

Thus fluids motion will be governed by the form in which applied forces, deformations and dynamic viscosity are related to each other. Experiments enable to obtain mathematical correlations between these variables known as constitutive equations

which in general, describe linear and non linear behaviors. The simplest form of constitutive equation is the one defined by the so called (*Newton viscous law*), which describes a linear behavior in which viscosity is a constant independent of deformations rates. This kind of fluids are also known as *Newtonian fluids*. For more complex fluids or *Non Newtonian fluids*, viscosity (*strictly apparent viscosity*) will be influenced by rate of deformation at each point of space leading to non linear models. Substances like water, air and simple oil derivatives are to some extent good examples of linear fluids, while blood, ink, mud or honey are common examples of non Newtonian fluids.¹

1.2 Mathematical Description of Newtonian Fluids Motion

From a macroscopic point of view, fluids can be considered as a collection of *material particles* several orders of magnitude larger than molecules free path. This approach known as *Continuum Hypothesis* enables to describe mechanical and thermodynamic magnitudes in terms of continuous functions. The mathematical description of fluids motion is entirely defined when the velocity and two thermodynamic variables, usually pressure and density, are known [1]. Furthermore, macroscopic description of fluids motion requires that conservation laws of mass, momentum and energy would be satisfied according to the principles of Continuum Mechanics. This approach even though simplifies physical understanding leads to complex systems of partial differential equations. To describe Newtonian fluids that will be the subject of study in the present work, several relations must be defined.

¹Constitutive equations are the field of research of *Rheology*

Constitutive Equation for Newtonian Fluids

As it was mentioned before, Newtonian fluids exhibit a linear relationship between external forces and deformations through time while dynamic viscosity remains constant. In order to address this constitutive equation for a Newtonian fluid, let's consider the one dimensional situation presented in figure (1.1). In this case the upper plate moves at a constant velocity along the x - direction while the bottom plate remains at rest. Space between the two plates is filled with a Newtonian fluid which exhibit a linear velocity distribution while deformation takes place (*linear behavior*). Both plates have constant area (A) in contact with the fluid through which external force is applied. Dynamic viscosity makes fluids layers to have the same velocity of the surfaces in contact. (*This is a boundary condition known as non slip*).

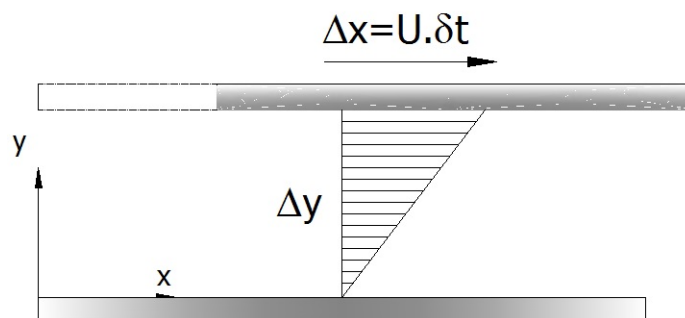


Figure 1.1: Schematic Diagram of Viscous Experiment

A measure of the angular deformation can be defined as follows:

$$\theta = \frac{\Delta x}{\Delta y} \quad (1.1)$$

or more conveniently,

$$\theta = \frac{\Delta u \delta t}{\Delta y} \quad (1.2)$$

Noting that angular deformation increases with time, and is proportional to external forces δF , distribution over plates area δA enables to determine a relationship between variables as follows:

$$\left(\frac{\delta F}{\delta A} \right) \propto \frac{\Delta x}{\Delta y \delta t} \quad (1.3)$$

Then an equation is obtained by replacing the proportionality for a constant which turns out to be the dynamic viscosity. Then a constitutive equation for Newtonian fluids is expressed as:

$$\tau_{yx} = \mu \frac{\partial u}{\partial y} \quad (1.4)$$

where $\frac{\partial u}{\partial y}$ represents the velocity gradient perpendicular to velocity direction known as *rate of strain*, and τ_{yx} is the shear stress in the direction of the flow.

An extension of previous results for multidimensional flows is given by Stokes viscous law [2], in which Cauchy stress tensor is related to strain tensor by means of a constant viscosity. In Cartesian coordinates stress tensor components are related to the rate of strain and viscosity as follows:

$$\tau_{xx} = -p + 2\mu \frac{\partial u}{\partial x} \quad \tau_{yy} = -p + 2\mu \frac{\partial v}{\partial y} \quad \tau_{zz} = -p + 2\mu \frac{\partial w}{\partial z} \quad (1.5)$$

$$\tau_{yx} = \mu \left(\frac{\partial u}{\partial y} + \frac{\partial v}{\partial x} \right) \quad \tau_{zx} = \mu \left(\frac{\partial u}{\partial z} + \frac{\partial w}{\partial x} \right) \quad \tau_{yz} = \mu \left(\frac{\partial v}{\partial z} + \frac{\partial w}{\partial y} \right) \quad (1.6)$$

where shear stresses are symmetric so $\tau_{xy} = \tau_{yx}$, $\tau_{xz} = \tau_{zx}$, $\tau_{yz} = \tau_{zy}$ and thermodynamic pressure (*which for incompressible fluids is represented by hydrostatic pressure*), accounts for a spherical component of the stress state. A general expression in tensor form of constitutive equation for Newtonian incompressible fluids is:

$$\tau_{ij} = -p \delta_{ij} + \mu \left(\frac{\partial V_i}{\partial x_j} + \frac{\partial V_j}{\partial x_i} \right) \quad (1.7)$$

Conservation Principle for Newtonian Fluids

Fluids motion is governed by conservation principles for mass, linear and angular momentum and energy . The Continuum Mechanics approach requires for conservation principle to be develop in such a form, that continuous changes in variables can be tracked through space and time. This approach leads to the following partial differential equations:

For conservation of mass,

$$\nabla \cdot (\rho V) + \frac{\partial \rho}{\partial t} = 0 \quad (1.8)$$

where ∇ *Nabla* operator is expressed in the appropriate coordinate system, V is fluid velocity field and ρ is the density of the fluid.

On the other hand, linear momentum equation requires a relation between applied forces on continuum boundaries and particles acceleration.

$$\nabla \cdot \tau + f_b = \rho \frac{DV}{Dt} \quad (1.9)$$

Here $\frac{DV}{Dt}$ represents the material or *Lagrangian* description of acceleration, f_b are the body forces and τ the stress tensor field. On the hand, in the spatial or *Eulerian* description motion, each velocity component is represented by a scalar function of space and time,

$$\vec{V} = u(x, y, z, t)\vec{i} + v(x, y, z, t)\vec{j} + w(x, y, z, t)\vec{k}$$

and acceleration is described by the following expression.

$$\vec{a} = \frac{\partial \vec{V}}{\partial t} + \vec{V} \cdot \nabla \vec{V} \quad (1.10)$$

Then replacing equation (1.2) and (1.5) onto (1.4), the final form of momentum equation for Newtonian fluids known as (*Navier Stokes equation*) is obtained.²

$$-\nabla p + \mu \nabla^2 V + f_b = \rho \left(\frac{\partial V}{\partial t} + V \cdot \nabla V \right) \quad (1.11)$$

Expressions (1.7) and (1.11) constitute a consistent system of four non linear partial differential equations, for which in the case of incompressible flows, *pressure* p and *velocity components* u, v, w are the unknown variables, while density ρ and dynamic viscosity μ are known constant a priori. Analytic solutions for this system of equations does not exist for the general case. However, many solutions have been developed for special cases of interest under appropriate assumptions. Analysis of confined fluids flow through ducts of different shapes is to some extent part of these special family of solutions. [4]

1.3 Laminar Viscous Flow Through Tubes of Elliptic Cross Section

One of the first applications of viscous flow model through confined or bounded regions, is the one related to pressure driven flows throughout tubes. To determine velocity profile and pressure changes throughout a tube of given section, Navier Stokes equation must be solved and proper boundary conditions must be applied. For two dimensional fully developed, steady state flow throughout an straight tube, Navier Stokes equation simplifies to the following form:

²This equation was first derived by *Claude Louis Navier and George Gabriel Stokes* independently and to the present day, remains as one of the most famous, elegant and also intriguing equations of Physics.

$$\nabla^2 u = \frac{1}{\mu} \frac{\partial p}{\partial x} \quad (1.12)$$

where $u(z, y)$ is the velocity component in the x-direction, accelerations are not present and body forces are neglected. On the other hand, continuity equation must be satisfied to assure mass conservation, which in this case is satisfied by means of a trivial form of the equation,

$$\nabla u = 0 \quad (1.13)$$

Solutions for Elliptic Cross Section

In order to present a general methodology for the analysis of confined viscous flows throughout tubes of different geometries, a first example is developed over a constant elliptic cross section. This first analysis *which can also be applied to cylindrical cross sections*, has the purpose to establish the methodology for further more complex analysis in duct with varying cross section as will be developed later on.

The analysis is carried out by means of coordinates transformations of *mapping*(z,y) coordinates onto (η, ξ) space as follows:

$$\eta = \frac{y}{a}, \quad \xi = \frac{z}{b} \quad (1.14)$$

where a and b are the length of ellipses semi axis as shown in figure 1.2

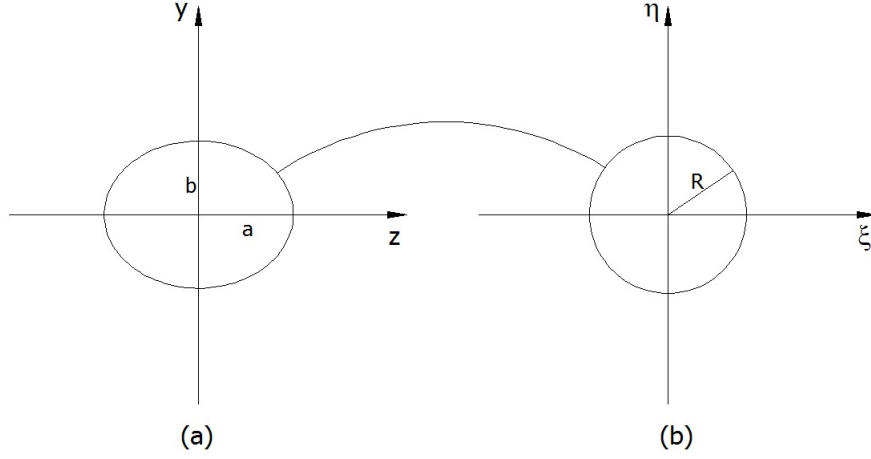


Figure 1.2: Elliptical cross section mapped onto cylindrical space

Considering that the mapping process transforms an elliptic domain into a circular one, solution of Poisson equation is developed by another transformation into cylindrical coordinates as follows:

$$\eta = r \cos \theta, \quad \xi = r \sin \theta \quad (1.15)$$

where $0 < r < R$.

Then the final form of the equation is:

$$\frac{1}{r} \frac{\partial}{\partial r} \left(r \frac{\partial u}{\partial r} \right) = \frac{1}{\mu} \frac{\partial p}{\partial x} \quad (1.16)$$

Noting that pressure gradient ∇p is not a function of radial coordinate, equation (1.12) can be integrated in a straightforward manner and adequate boundary conditions can be evaluated as follows:

$$u(r) = \frac{1}{4\mu} \frac{\partial p}{\partial x} (r^2) + C_1 \ln(r) + C_2 \quad (1.17)$$

$$\left. \frac{\partial u}{\partial r} \right|_{r=0} = 0 \longrightarrow C_1 = 0$$

$$u(R) = 0 \longrightarrow C_2 = -\frac{1}{4\mu} \frac{\partial p}{\partial x} (R^2)$$

The final form of the solution for the velocity distribution considering $R = 1$ is:

$$u(r) = \frac{1}{4\mu} \frac{\partial p}{\partial x} (1 - r^2) \quad (1.18)$$

Which is the solution for a cylindrical cross section. Moreover, for a tube of elliptical cross section in which the boundary is defined as

$$\frac{y^2}{a^2} + \frac{z^2}{b^2} = 1 \quad (1.19)$$

the momentum equation is satisfied by the following expression.

$$u(y, z) = \frac{1}{2\mu} \frac{\partial p}{\partial x} \frac{(ab)^2}{a^2 + b^2} \left(1 - \left(\frac{y}{a} \right)^2 - \left(\frac{z}{b} \right)^2 \right) \quad (1.20)$$

in which velocity vanishes at every point on the tubes wall. Moreover since

$$\frac{\partial^2 u}{\partial y^2} = \frac{2}{a^2} \left[\frac{1}{2\mu} \frac{\partial p}{\partial x} \frac{(ab)^2}{a^2 + b^2} \right] \quad (1.21)$$

and

$$\frac{\partial^2 u}{\partial z^2} = \frac{2}{b^2} \left[\frac{1}{2\mu} \frac{\partial p}{\partial x} \frac{(ab)^2}{a^2 + b^2} \right] \quad (1.22)$$

it is clear that

$$\frac{\partial^2 u}{\partial y^2} + \frac{\partial^2 u}{\partial z^2} = \frac{1}{\mu} \frac{\partial p}{\partial x} \quad (1.23)$$

satisfies the momentum equation. Extension of the present method to more general cross sections can be achieved by means of Complex Variable methods. Some results are presented in figure 1.3

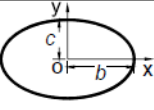
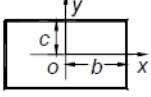
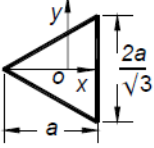
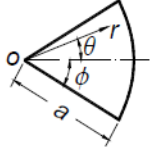
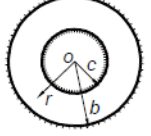
cross-section	Area, Perimeter	mean velocity (analytical) \bar{w}	$fRe\sqrt{A}$
	$A = \pi bc$ $P = 4bE(\sqrt{1-\epsilon^2})$	$\frac{c^2}{4(1+\epsilon^2)} \frac{\Delta p}{\mu L}$	$\frac{2\pi\sqrt{\pi}(1+\epsilon^2)}{\sqrt{\epsilon}E(\sqrt{1-\epsilon^2})}$
	$A = 4bc$ $P = 4(b+c)$	$\frac{\Delta p c^2}{\mu L} \left[\frac{1}{3} - \frac{64c}{\pi^5 b} \tanh\left(\frac{\pi b}{2c}\right) \right]$	$\frac{12}{\left[1 - \frac{192}{\pi^5} \epsilon \tanh\left(\frac{\pi}{2\epsilon}\right) \right] (1+\epsilon) \sqrt{\epsilon}}$
	$A = a^2/\sqrt{3}$ $P = 6a/\sqrt{3}$	$\frac{1}{60} \frac{\Delta p a^2}{\mu L}$	$\frac{20}{3^{1/4}} = 15.197$
	$A = \phi a^2$ $P = 2a(1+\phi)$	$\frac{\Delta p a^2}{\mu L} g(\phi)^{[1]}$	$\frac{\phi\sqrt{\phi}}{(1+\phi)g(\phi)^{[1]}}$
	$A = \pi(b^2 - c^2)$ $P = 2\pi(b+c)$	$\frac{\Delta p b^2}{8\mu L} \left(\epsilon^2 - 1 + \frac{2 \ln(1/\epsilon) + \epsilon^2 - 1}{\ln(1/\epsilon)} \right)$	$\frac{8\sqrt{\pi}(1-\epsilon)\sqrt{1-\epsilon^2}}{\left(\epsilon^2 - 1 + \frac{2 \ln(1/\epsilon) + \epsilon^2 - 1}{\ln(1/\epsilon)} \right)}$
${}^1g(\phi) = \frac{\tan(2\phi) - 2\phi}{16\phi} - \frac{128\phi^3}{\pi^5} \sum_{n=1}^{\infty} \left[\frac{1}{(2n-1)^2(2n-1+4\phi/\pi)^2(2n-1-4\phi/\pi)} \right]$			$\epsilon = c/b$

Figure 1.3: Analytic solutions for some cross section. Ref.[4]

From velocity distribution three important parameters can be determined for all problems which are: *flow rate*, *pressure variation* and *shear stress* at the wall as follows:

Flow Rate

Flow rate defined as the amount of volume moving through section is defined as,

$$q = \int u \hat{n} dS \quad (1.24)$$

where \hat{n} is the unit vector normal to the flow surface S. Integration of equation (1.15)

over an elliptic cross section defines the flow rate as follows.

$$q = 4 \int_0^a \int_0^{\frac{b\sqrt{a^2-y^2}}{a}} \left[\frac{1}{2\mu} \frac{\partial p}{\partial x} \frac{(ab)^2}{a^2 + b^2} \left(1 - \left(\frac{y}{a} \right)^2 - \left(\frac{z}{b} \right)^2 \right) \right] dz dy \quad (1.25)$$

Here integration has been developed over a quarter of the cross section, leading to the following expression,

$$q = \frac{1}{4\mu} \frac{\partial p}{\partial x} \frac{(ab)^3}{a^2 + b^2} \quad (1.26)$$

Pressure Variation

Equation (1.26) can be rearranged in terms of pressure drop for a tube of a given length (L),

$$\Delta p = \frac{4q\mu L(a^2 + b^2)}{(ab)^3} \quad (1.27)$$

which is the elliptic version of the well known *Hagen and Poiseuille* equation for pressure variation of laminar flow across ducts

Shear Stress

Shear stress exerted on the tube wall by the fluid can be determine by equation (1.6).

Considering the case of an elliptic cross section, the resulting shear is as follows:

$$\tau_{yx} = \mu \frac{\partial u}{\partial y} \quad , \quad \tau_{zx} = \mu \frac{\partial u}{\partial z} \quad (1.28)$$

and by the fact that

$$\tau_{\hat{n}x} = \frac{\mu}{ds} \left(\frac{\partial u}{\partial y} dy + \frac{\partial u}{\partial z} dz \right) \quad (1.29)$$

where s is the arc length of the elliptical boundary. From equation (1.20) and (1.26) we can write.

$$\mu \frac{\partial u}{\partial y} = -\frac{\partial p}{\partial x} \frac{b^2}{a^2 + b^2} y = -4\mu q \frac{y}{a^3 b} \quad (1.30)$$

$$\mu \frac{\partial u}{\partial z} = -\frac{\partial p}{\partial x} \frac{a^2}{a^2 + b^2} z = -4\mu q \frac{z}{ab^3} \quad (1.31)$$

Also from (1.19) and the definition of arc length we have,

$$\frac{dy}{ds} = \frac{a^2 z}{\left(a^4 z^2 + b^4 y^2\right)^{1/2}}, \quad \frac{dz}{ds} = \frac{b^2 y}{\left(a^4 z^2 + b^4 y^2\right)^{1/2}} \quad (1.32)$$

Finally, from equations (1.29),(1.30), (1.31) and (1.32), the following expression for shear stress is obtained,

$$\tau_{\hat{n}x} = -\frac{4\mu q}{\left(a^4 z^2 + b^4 y^2\right)^{1/2}} \frac{2yz}{ab} \quad (1.33)$$

Poiseuille Number

To extend the analytic results to more general shapes, solutions for laminar viscous flow can be expressed as a function of the friction factor and Reynolds number. Lets consider Darcy-Weisbach equation obtained by means of dimensional analysis,

$$\Delta p = f \cdot \frac{\rho L U^2}{L_c} \frac{1}{2} \quad (1.34)$$

equating (1.27) and (1.30) and re arranging terms, a new parameter known as Poiseuille number can be obtained.

$$f \cdot Re = \frac{8L_c^2 (\pi^{1/2}) (a^2 + b^2)}{(ab)^2} \quad (1.35)$$

This non dimensional number is usually expressed in terms of the Fanning's friction factor C_f , and an alternative characteristic length L_c . [3].

Noting that equation (1.35) expresses Poiseuille number in term of geometric parameters and pressure gradient which can be determined by numerical procedures, a general method can be applied to arbitrary shapes by means of numerical solutions of equation (1.12). The following chapter is devoted to explore numerical solutions to the laminar viscous flow problem.

Chapter 2

Numerical Solution for Laminar

Viscous Flow Through Tubes of Varying

Cross Section

Numerical methods are powerful tools for research and design purposes in modern Fluid Dynamics. The fundamental idea behind these methods is to transform partial differential equations *PDE* onto some equivalent discrete system of algebraic equations, in which unknown variables are determined for a finite number of point inside the domain. The process of transforming PDE equations onto its discrete equivalents in Fluid Dynamics, is usually carried out by means *Finite Differences* or *Finite Volumes* methods. However, noting that the problem is defined by an elliptic PDE with boundary conditions well defined at every point on the contour, implementation of *finite element method* is to some extent straightforward.¹

¹A problem in which boundary conditions are defined on a complete contour enclosing the region is known as *boundary value problem*. *Finite Element Method* is particularly well posed to address such a *PDE* problems.[6]

It is important to emphasize that numerical solutions for the elliptic PDE that arises in the context of fluids flow throughout a tube, are valid for any cross section regardless its shape. The main reason for this lies on the fact that the model is intended for arbitrary *constant* cross sections. However, for the case of flows throughout *varying* cross sections, a different approach considering inertial effects is required.

2.1 Numerical Solution for Laminar Viscous Flow Through Tubes of Arbitrary Constant Cross Section

Numerical solutions for laminar flows across tubes of arbitrary constant cross section, are developed by means of a non dimensional form of equation (1.12) as follows:

$$\hat{\nabla}^2 \hat{u} = -1 \quad (2.1)$$

in which non dimensional transformations for pressure, velocity and geometry are defined as [1].

$$\hat{p} = \frac{p}{\rho U^2}, \quad \hat{y} = \frac{y}{L_y}, \quad \hat{z} = \frac{z}{L_z}, \quad \hat{u} = -\mu \frac{u}{R^2 \nabla p}, \quad \hat{v} = \frac{v}{U}, \quad \hat{w} = \frac{w}{U} \quad (2.2)$$

Here U is the average velocity in the flow direction x and $L_y = L_z = R$, in which R is the characteristic length of the cross section generally represented by the *i.e. Hydraulic Diameter*, or also defined as the square root of area [3].² Equation (2.1) is an elliptic PDE which numerical solutions may be obtained for any cross section by means of Finite Element Method.

²The use of a single parameter L_c to scale all dimensions, is based on the assumption of fully developed flow regime.

For the case of arbitrary varying cross sections, numerical methods must be adjusted to take into account the effect of acceleration throughout the tube as it is done in the context of *lubrication approximation* and *perturbation theory*, as shown in chapter 3. All the mentioned strategies have similar limitations when steep variations of cross sections are present. Nevertheless, taking advantage of the versatility of numerical methods, an approach to the solution of laminar flows across arbitrary varying cross section is explored in section (2.3). In what follows, general derivation of the finite element method applied to the problem in question is presented.

2.2 Numerical Solutions by Finite Element Method

The fundamental idea behind finite element method is to construct an approximation to the solution of a partial differential equation, by means of piece wise interpolation functions for the unknown variables.

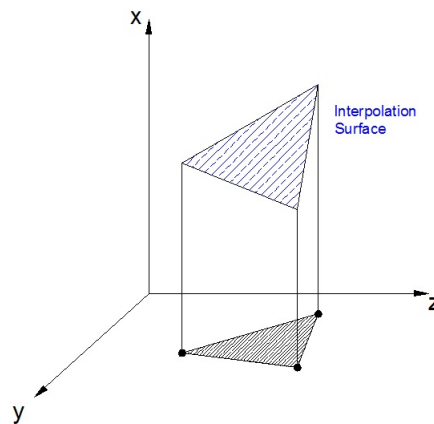


Figure 2.1: Interpolation surface in finite element solution

Such interpolation functions will be in general polynomials of appropriate order under the rules of interpolation. These functions known as *shape functions* h_i , will be

defined on a *local coordinate system* [r,s] in the domain[0,1].

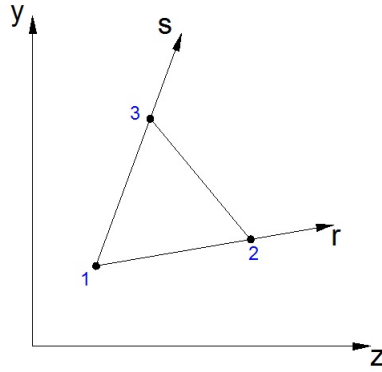


Figure 2.2: Coordinates mapping

On the other hand, in order to find the best approximation to the solution function, a minimization criteria for residual values *errors* for the approximation must be defined. In this case the weighted residual approximation or *Galerkin approximation* which carries on the process by means of the same shape functions will be applied. *Isoparametric formulation.*

Lets consider an approximation function for the velocity field defined in terms of

$$\hat{u} = \sum_{i=1}^N h_i \hat{u}_i \quad (2.3)$$

and the mapping functions between global and local set of coordinates (y,z) and r(y,z), s(y,z) as,

$$\hat{y} = \sum_{i=1}^N h_i \hat{y}_i, \quad \hat{z} = \sum_{i=1}^N h_i \hat{z}_i \quad (2.4)$$

in which h_i are the shape functions intended for interpolation of unknown variables.

Considering a linear triangular finite element, shape functions are defined as,

$$h_1 = r \quad h_2 = s \quad h_3 = 1 - r - s \quad (2.5)$$

Moreover, replacing the approximation function (2.3) onto (2.1) a residual is generated. Furthermore, taking into account the relative weight of every local residual generated by means of the shape functions, the following general expression can be determined.

$$\int_{\Omega} \left[(\hat{\nabla}^2 \hat{u} + 1) h_i d\Omega \right] = 0 \quad (2.6)$$

which integrated by parts leads to the following expression:

$$\int_{\Omega} \hat{\nabla} (h_i \hat{\nabla} \hat{u}_i) d\Omega - \int_{\Omega} \hat{\nabla} \hat{h}_i \hat{\nabla} \hat{h}_j \hat{u}_j d\Omega - \int_{\Omega} h_i d\Omega = 0 \quad (2.7)$$

First integral on equation (2.7) can be expressed in terms of a line integral by means of Gauss theorem which leads to the following expression,

$$\int_{\Gamma} (h_i \hat{\nabla} \hat{h}_j \hat{u}_j) \hat{n} dS - \int_{\Omega} \hat{\nabla} \hat{h}_i \hat{\nabla} \hat{h}_j \hat{u}_j d\Omega - \int_{\Omega} h_i d\Omega = 0 \quad (2.8)$$

Then, considering that velocity is zero at tube's wall *non slip boundary condition*, surface integral in (2.7) vanishes leading to a linear system of equations of the form

$$K_{ij} \hat{u}_j = f_i \quad (2.9)$$

in which,

$$K_{ij} = \sum_{n=1}^{Ne} \left(\int_{\Omega} \hat{\nabla} \hat{h}_i \hat{\nabla} \hat{h}_j d\Omega \right), \quad f_i = \sum_{n=1}^{Ne} \left(\int_{\Omega} h_i d\Omega \right) \quad (2.10)$$

are the coefficients matrix K_{ij} and the solution vector f_i respectively.

Solution of system (2.9) enables to determine the velocity at every point of the mesh approximating the cross section of the tube. Proper velocity values for each node of the mesh can be determined re scaling the numerical solution. Moreover, flow rate and pressure variations along the tube can be determined by the same procedures described in section (1.3). Unit velocity distribution for different cross sections and the correspondent maximum velocities are presented in figure (2.3) and table (2.1) respectively.

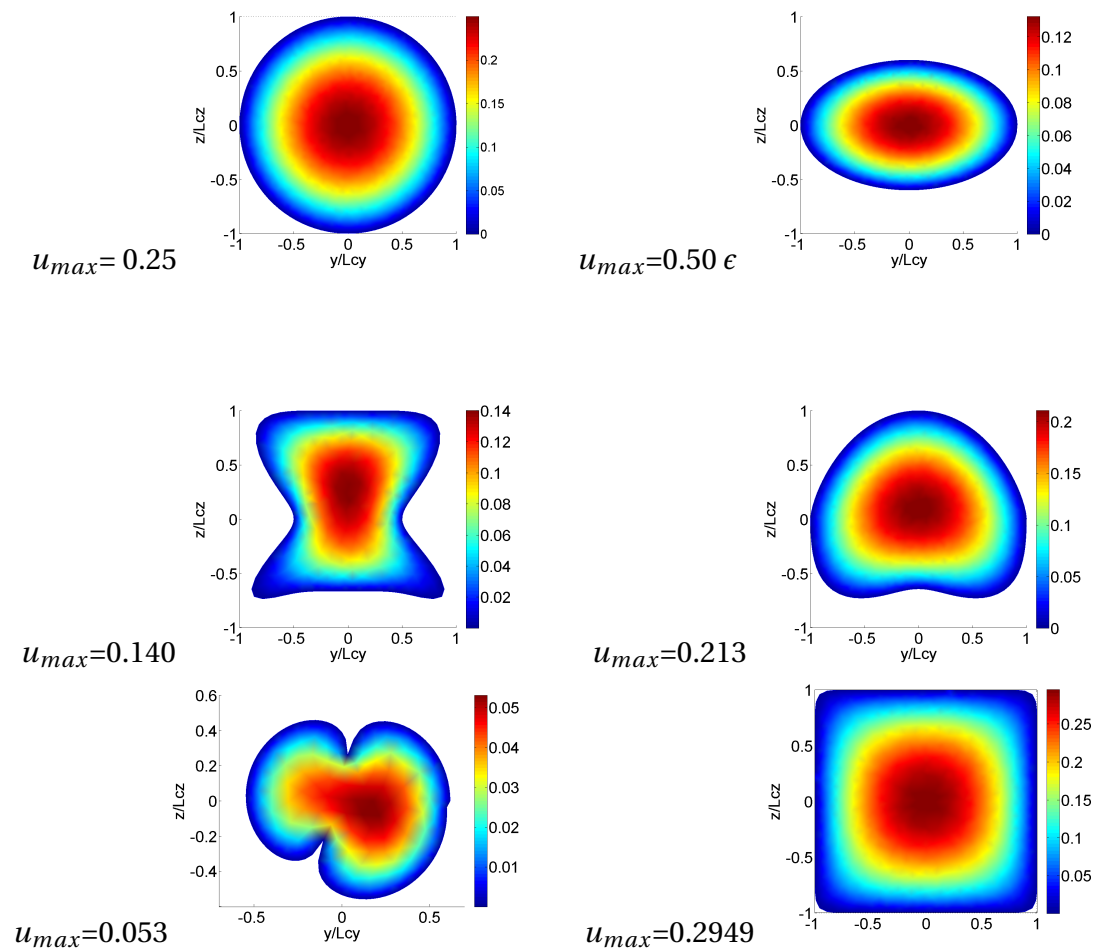


Figure 2.1: Unit velocity distribution for different cross sections and maximum unit value where u obtained by numerical analysis. $\epsilon = b^2 / (a^2 + b^2)$

Numerical solutions enable to calculate important hydrodynamic parameters such as pressure gradients and Poiseuille numbers for more general sections. Deduction of these relation are presented in the following section in the context of numerical perturbation approximations. In table 2.1 hydrodynamic parameters for simple cross sections are presented.

Cross Section	Analytic		Numerical		Analytic	Numerical
	u_{max}	$fRe_{\sqrt{A}}$	u_{max}	$fRe_{\sqrt{A}}$	τ_{mean}	τ_{mean}
Ellipse (b/a)						
1	0.2500	14.179	0.2500	14.196	0.5000	0.4915
3/4	0.1800	14.931	0.1799	14.580	0.4252	0.4222
1/2	0.1000	16.246	0.1000	15.332	0.3285	0.3312
1/4	0.0294	22.273	0.02939	22.495	0.1883	0.1959
Quadrilateral (b/a)						
1	0.2916	14.132	0.2949	13.964	0.5564	0.5011
3/4	0.2100	14.568	0.2110	14.540	0.4003	0.4245
1/2	0.1140	16.457	0.113	16.753	0.3153	0.3439
1/4	0.0314	22.77	0.031	28.35	0.1737	0.2000
Equilateral Triangle	0.0277	15.197	0.0279	17.505	0.1407	0.1487

Table 2.1: Analytic and numerical results for some known cross sections

2.3 Flow Through Arbitrary Varying Cross Section - Numerical Solutions

The procedure described in what follows takes advantage of numerical methods to determine the pressure gradient of a flow across tubes of arbitrary varying cross section. In this case, the influence inertia (*convective acceleration*) can not be neglected and different approaches are developed to address this condition. For slow variations of cross section shapes along tube length (*where definition of smooth variation is not always straightforward*), axial convective acceleration component may be included in classical models by means of *perturbation approximations*, which are extensively applied in the field of Fluid Mechanics.

Analytic solutions by means of perturbation approximations are known for simple shapes and are presented in detail for an elliptic section in chapter 3. As it will be shown, correction of pressure gradients obtained by means of numerical perturbations will be independent of section shapes but dependent on axial changes of it. Therefore, once numerical solutions as presented in section 2.2 are obtained for an specific section, and adequate perturbation function is determined from the acceleration term, solutions for different cross sections are to some extent straightforward. Considering the convective acceleration component in the flow direction and changes in size of cross section along the tube, perturbation can be expressed as follows,

$$\epsilon \rho u \frac{\partial u}{\partial x} = \epsilon \rho \frac{q^2}{A_{(x)}^3} \frac{dA_{(x)}}{dx} \quad (2.11)$$

where perturbation ϵ is given by the quotient between characteristic length of cross

section and total length along the tube.

In what follows, two approaches are explored to address the effect of convective acceleration from a different perspective. This approaches exhibit satisfactory results considering their simplicity compared to analytic procedures explained in chapter 3.

2.4 Alternative Numerical Perturbation

The procedures detailed in this section have the purpose to explore alternative solution strategies to address the convective acceleration components in a more general way. The advantage of the proposed approaches lies on the fact that cross section changes and their effect on velocity components, can be included in the mathematical structure of numerical method enabling the solution of a broader range of cases.

The first approach which will be identified as *alternative perturbation*, operates over axial velocity component in the viscous as well as in the convective term, and assuming that transverse components of convective acceleration are negligible. This approach is closely related to the analytic perturbation procedure explained in chapter 3. The second approach identified as *Convective Transverse Correction*, includes the effect of transverse acceleration component on axial velocity.

Alternative Perturbation

Consider again equation (1.7) but in this case with the acceleration component *convective acceleration* in the flow direction as follows,

$$\nabla^2 u = \frac{1}{\mu} \frac{\partial p}{\partial x} + \frac{\rho}{\mu} u \frac{\partial u}{\partial x} \quad (2.12)$$

Transforming equation (2.1) into a non dimensional form by means of equations (2.2) and expressing velocity in terms of flow rate and cross area function, equation (2.10) turns into the following form:

$$\hat{\nabla}^2 \hat{u} = -1 + \frac{\rho \nabla p L_c^2 q}{\mu \nabla p} \hat{u} \frac{\partial A(x)}{\partial x} \quad (2.13)$$

in which \hat{u} is a non dimensional velocity, L_c a characteristic length. Then, calculating the derivative of area function leads to the following expression,

$$\frac{\rho L_c^2 q \hat{u}}{\mu} \frac{\partial A(x)}{\partial x} = - \left(\frac{\rho U L_c}{\mu} \right) \left(\frac{L_c A'(x)}{A_{(x)}^{1/2}} \right) \hat{u} \quad (2.14)$$

in which $A'_{(x)}$ is the derivative of the area function with respect to x- coordinate which is the *axial axis*. After some arrangements a final form of the flow equation as a function of Reynolds number, section area function and characteristic length is obtained.

$$\hat{\nabla}^2 \hat{u} = -1 - \left(\frac{\rho U L_c}{\mu} \right) \left(\frac{L_c A'(x)}{A_{(x)}} \right) \hat{u} \quad (2.15)$$

In equation (2.14) characteristic length is defined as the square root of section area $L_c = \sqrt{A(x)}$ or alternatively, the hydraulic radius, which are applied as reference magnitudes for hydrodynamic calculations. Then considering the values that the product of Reynolds number times local cross section area can take, enables to address

the relative weight that acceleration has in the momentum equation. In this way, perturbation parameter is defined as $\epsilon = L_c A'(x)/(A(x))$.

Regular perturbations are defined by series expansion of the variable of interest with power increments of ϵ . For the present case, axial component of non dimensional velocity is developed in a series expansion with an small increment ϵ leading to a non dimensional perturbed form of Navier Stokes equation.

$$\hat{\nabla}^2(\hat{u}_o + \epsilon \hat{u}_1) = -1 - Re\left(\frac{L_c A'(x)}{A(x)}\right)(\hat{u}_o + \epsilon \hat{u}_1) \quad (2.16)$$

By expanding and arranging terms with the same perturbation order, a system of partial differential equations is obtained.

$$\hat{\nabla}^2(\hat{u}_o) = -1 \quad (2.17)$$

$$\epsilon \hat{\nabla}^2(\hat{u}_1) = -\epsilon R \hat{u}_o$$

$$\epsilon^2 A \hat{u}_1 = 0$$

$$\text{where } R = Re\left(\frac{L_c A'(x)}{A(x)}\right).$$

Noting that equations for u_o and u_1 are elliptic Poisson equations, numerical solutions are possible for many section shapes. Moreover, considering that perturbed values of velocity must be calculated at the same nodal point in the finite element mesh, a common stiffness matrix will be obtained for both systems. Solution vectors will differ between each other in a constant value of the form $R \hat{u}_o$. This observation enables to solve in a numerical form, one system of equation with multiple solution vectors.

Considering the procedure developed in section (2.2), velocity can be solved as follows:

$$\hat{u}_o = K_{ij}^{-1} f_i \quad (2.18)$$

and

$$\hat{u}_1 = K_{ij}^{-1} R \hat{u}_o \quad (2.19)$$

in which solution vector f in the perturbed equation has been scaled by $R \hat{u}_o$.

Finally, velocity distribution at each point of each cross section is expressed as a series of the form:

$$\hat{u} = K_{ij}^{-1} f_i + \epsilon K_{ij}^{-1} R \hat{u}_o \quad (2.20)$$

From numerical solution expressed in (2.19) flow rate and pressure gradient can be determined for any given section by means of integration. It is important to notice that the integration process is carried out over each finite element area A_e , which is rescaled by a characteristic length L_c , leading to the following relation: $dA(x) = L_c^2 dA_e$

Details of the procedure are presented in what follows. First, flow rate is expressed in terms of dimensionless velocity (2.18) and transformation (2.2).

$$q = \sum_e \int \frac{L_c^4 (-\nabla p)}{\mu} \left[\sum_e K_{ij}^{-1} f_i + \epsilon \sum_e K_{ij}^{-1} R \hat{u}_{oi} \right] dA_e \quad (2.21)$$

Then, replacing equation (2.17) and (2.18) in (2.19), pressure gradient is expressed as,

$$\nabla p = - \frac{q \mu}{L_c^4 \int \left[\sum_e K_{ij}^{-1} f_i + \epsilon \sum_e K_{ij}^{-1} R e \hat{u}_o \right] dA_e} \quad (2.22)$$

Equation (2.22) represents the local pressure gradient for each section of the tube from which pressure function can be determined. *Results for this procedure are presented in chapter 4.* Moreover, equation (2.22) can be compared to Darcy Weisbach equation *in terms of Fanning skin coefficient C_f* , to obtain the Poiseuille number as follows,

$$\Delta p = - \int \left[\frac{q\mu}{(L_c^4) \left[\sum_e K_{ij}^{-1} f_i + \epsilon \sum_e K_{ij}^{-1} Re \hat{u}_{oi} \right] dA_e} \right] dx \quad (2.23)$$

$$\frac{\Delta p}{\gamma} = \int \left[\frac{q\mu}{L_c^4} + \frac{1}{\gamma\beta} \right] dx = f \cdot \frac{dx}{L_c} \frac{1}{2g} U^2 \quad (2.24)$$

where U is the mean velocity and a new variable β defined as $\beta = f \left[\sum_e K_{ij}^{-1} f_i + \epsilon \sum_e K_{ij}^{-1} Re \hat{u}_{oi} \right]$.

Considering Reynolds number, expressing mean velocity in terms of flow rate and rearranging terms in (2.24), leads to

$$\frac{q\mu}{\beta L_c^4} = f \cdot \frac{\rho L_c}{L_c^2} \frac{q^2}{2A_{(x)}^2} \quad (2.25)$$

and an expression for numerical Poiseuille number is defined as follows,

$$f \cdot Re = \frac{2A_{(x)}}{\beta L_c^2} \quad (2.26)$$

Expression (2.25) combined with Darcy Weisbach equation, enables to calculate pressure drop for any arbitrary cross section as long as Reynolds number and hydraulic radius are known. On the other hand, by adding the numerical lubrication part of (2.23) to results from analytic perturbations as presented in chapter 3, classical perturbations solutions can be developed. Differences between these two approaches are presented in the examples developed in chapter 4.

Convective Acceleration Correction

Lets consider Navier Stokes equation in the flow direction with the entire acceleration term as follows:

$$\mu \nabla^2 u = \nabla p + \rho \left(u \frac{\partial u}{\partial x} + v \frac{\partial u}{\partial y} + w \frac{\partial u}{\partial z} \right) \quad (2.27)$$

Considering that transverse component of velocity are not strictly null for varying cross sections, an strategy is developed to take into account their effect. For this purpose the basic assumptions established for lubrication approximations are again valid,

$$\frac{U}{Lc_{\hat{x}}} \sim \frac{V}{L_{\hat{y}}} \sim \frac{W}{L_{\hat{z}}} \quad (2.28)$$

where U,V,W are mean values of velocity components in the x,y,z direction respectively and

$$\frac{V}{U} \ll 1 \quad , \quad \frac{W}{U} \ll 1 \quad (2.29)$$

Transforming equation (2.27) into a non dimensional form by means of equation (2.2) leads to the following result.

$$\hat{\nabla}^2 \hat{u} = -1 + \left(Re \cdot \epsilon \frac{A'_{(x)}}{A_{(x)}} \hat{u} + \rho V \frac{Lc_x^2}{\mu L_c} \frac{\partial \hat{u}}{\partial \hat{y}} + \rho W \frac{Lc_x^2}{\mu L_c} \frac{\partial \hat{u}}{\partial \hat{z}} \right) \quad (2.30)$$

Then replacing V and W in terms of U using (2.27) leads to the following relations for Reynolds numbers involved.

$$\frac{\rho V Lc_x}{\mu} \sim \frac{\rho U L_y}{\mu}, \quad \frac{\rho W L_z}{\mu} \sim \frac{\rho U Lc_x}{\mu} \quad (2.31)$$

Finally replacing (2.29) in (2.28) leads to the final form of the equation.

$$\hat{\nabla}^2 \hat{u} = -1 + Re \left(\epsilon \frac{A'_{(x)}}{A_{(x)}} \hat{u} + \frac{L_y}{Lc_x} \frac{\partial \hat{u}}{\partial \hat{y}} + \frac{L_y}{Lc_x} \frac{\partial \hat{u}}{\partial \hat{z}} \right) \quad (2.32)$$

Equation (2.32) includes the effect that transverse velocity components have over axial velocity, which enable corrections on pressure gradient. Solution of (2.32) by means of finite element method is presented in what follows. The procedure previously applied to (2.15) is again applicable to (2.32).

Additional matrix which will be called *convective matrix* H , is developed in what follows and included in the final form of finite element solution.

Considering Galerkin approximation for transverse velocity components, integral form of convective matrix is,

$$H_{\hat{y}} = \int_{\Omega} \left(h_i \frac{\partial h_j}{\partial \hat{y}} \hat{u}_j \right) dA_e \quad (2.33)$$

$$H_{\hat{z}} = \int_{\Omega} \left(h_i \frac{\partial h_j}{\partial \hat{z}} \hat{u}_j \right) dA_e \quad (2.34)$$

and

$$\left(K_{ij} - H_{\hat{y}ij} - H_{\hat{z}ij} \right) \hat{u}_o = -1 \quad (2.35)$$

$$\epsilon \left(K_{ij} - H_{\hat{y}ij} - H_{\hat{z}ij} \right) \hat{u}_1 = -\epsilon Re \hat{u}_o \quad (2.36)$$

Chapter 3

Laminar Flow Through Arbitrary

Varying Cross Section

Analytic solutions for laminar flows through tubes of arbitrary varying cross sections can be developed based on the hypothesis that *smooth variation of shape throughout tubes length* are present. Solution strategies to this problem can be developed by means of *lubrication approximation* and *asymptotic perturbations*.

3.1 Perturbation Approximation

As previously seen, lubrication approximation fails in the prediction of pressure variations for those cases in which changes in geometry are not sufficiently smooth for viscous forces to prevail over inertia. A correction of that procedure can be achieved by mean of the so called perturbation theory in which a *perturbation parameter* (ϵ) is defined as a correction factor on a power series.

$$V = \sum_{i=0} \left(u_i \epsilon^i, v_i \epsilon^i, w_i \epsilon^i \right) \quad (3.1)$$

$$p = \sum_{i=0}^{\infty} (p_i \epsilon^i) \quad (3.2)$$

The definition of the perturbation parameter is based on the relation between some characteristic length (a_o) for the cross section and the length (L) of the entire tube. Comparing the inertial and viscous terms in Navier Stokes equation a relation for perturbation parameter can be obtained as explained in (2.1). Therefore perturbation parameter takes the following form:

$$\epsilon = \frac{a_o}{L} \quad (3.3)$$

The analysis of flow problem by perturbation method implies the search for solutions of the Navier Stokes equation and mass conservation for a three dimensional flow in which, two velocity components are assumed to be small compared with axial velocity. A set of non dimensional variables for coordinates mapping, velocity components and pressure are defined considering the perturbation parameter.[4]

$$(\hat{x}, \hat{y}, \hat{z}) = \frac{1}{L}(xL, a_o y, a_o z) \quad (3.4)$$

$$\hat{V}(\hat{u}, \hat{v}, \hat{w}) = \frac{1}{U}(u, \epsilon v, \epsilon w) \quad (3.5)$$

$$\hat{p} = \left(\frac{\epsilon Re}{\rho U^2} \right) p \quad (3.6)$$

In these expressions U is the axial velocity and Re is the Reynolds number defined as the relation of Inertial forces to viscous forces expressed as:

$$Re = \frac{\rho U a_o}{\mu} \quad (3.7)$$

Solution for elliptic section follows to some extent what has been developed for a straight tube. Thus, coordinates mapping in expression (1.14) are applied considering that in this case the ellipsis semi axis (a, b) are functions of length, therefore $a = a(x)$ and $b = b(x)$.

Then transformation of mass conservation equation is as follows:

$$\frac{\partial u}{\partial x} + \frac{\partial v}{\partial y} + \frac{\partial w}{\partial z} = 0 \quad (3.8)$$

From this point on, mapping transformation are redefined as follows,

$$\eta = \frac{y}{a}, \quad \zeta = \frac{z}{b} \quad (3.9)$$

where u, v, w are functions of (x, η , ζ). Then, mapping process leads to the following dependencies:

$$Du = \frac{\partial u}{\partial x} + \frac{\partial u}{\partial \eta} \frac{\partial \eta}{\partial x} + \frac{\partial u}{\partial \zeta} \frac{\partial \zeta}{\partial x} \quad (3.10)$$

$$\frac{\partial \eta}{\partial x} = -\frac{y}{a^2} \frac{\partial a}{\partial x} \quad (3.11)$$

$$\frac{\partial \zeta}{\partial x} = -\frac{z}{b^2} \frac{\partial b}{\partial x} \quad (3.12)$$

Therefore equation (3.7) has the following form:

$$D = \frac{\partial}{\partial x} - \frac{\eta a'}{a} \frac{\partial}{\partial \eta} - \frac{\zeta b'}{b} \frac{\partial}{\partial \zeta} \quad (3.13)$$

in which D, a' b' are derivatives with respect to the x- component. Similar transformations enable the conversion of velocity components v and w as well:

$$\frac{\partial v}{\partial y} = \frac{\partial v}{\partial \eta} \frac{\partial \eta}{\partial y} = \frac{1}{a} \frac{\partial v}{\partial \eta} \quad (3.14)$$

$$\frac{\partial w}{\partial z} = \frac{\partial w}{\partial \zeta} \frac{\partial \zeta}{\partial z} = \frac{1}{b} \frac{\partial w}{\partial \zeta} \quad (3.15)$$

Then, final form of mass conservation equation mapped onto the new coordinates is:

$$Du + \frac{1}{a} \frac{\partial v}{\partial \eta} + \frac{1}{b} \frac{\partial w}{\partial \zeta} = 0 \quad (3.16)$$

By means of similar procedure each term in the momentum equation (Navier Stokes equation) is transformed. For the sake of clarity the equation is presented in an expanded shape using the original Cartesian coordinates: ¹

$$-\frac{\partial p}{\partial x} + \mu \left(\frac{\partial^2 u}{\partial x^2} + \frac{\partial^2 u}{\partial y^2} + \frac{\partial^2 u}{\partial z^2} \right) = \rho \left(u \frac{\partial u}{\partial x} + v \frac{\partial u}{\partial y} + w \frac{\partial u}{\partial z} \right) \quad (3.17)$$

$$-\frac{\partial p}{\partial y} + \mu \left(\frac{\partial^2 v}{\partial x^2} + \frac{\partial^2 v}{\partial y^2} + \frac{\partial^2 v}{\partial z^2} \right) = \rho \left(u \frac{\partial v}{\partial x} + v \frac{\partial v}{\partial y} + w \frac{\partial v}{\partial z} \right) \quad (3.18)$$

$$-\frac{\partial p}{\partial z} + \mu \left(\frac{\partial^2 w}{\partial x^2} + \frac{\partial^2 w}{\partial y^2} + \frac{\partial^2 w}{\partial z^2} \right) = \rho \left(u \frac{\partial w}{\partial x} + v \frac{\partial w}{\partial y} + w \frac{\partial w}{\partial z} \right) \quad (3.19)$$

Transformations are implemented as follows:

$$\frac{\partial p}{\partial x} = Dp \quad (3.20)$$

$$\frac{\partial p}{\partial y} = \frac{1}{a} \frac{\partial p}{\partial \eta} \quad (3.21)$$

$$\frac{\partial p}{\partial z} = \frac{1}{b} \frac{\partial p}{\partial \zeta}$$

where D is the operator as in equation (3.12). Then for inertial terms (*convective acceleration components*) a new operator I is defined as follows:

$$I = uD + \frac{v}{a} \frac{\partial}{\partial \eta} + \frac{w}{b} \frac{\partial}{\partial \zeta} \quad (3.22)$$

Viscous terms are developed over the u - component noting that have the same shape for v and w components as well.

$$\frac{\partial^2 u}{\partial x^2} = \frac{\partial}{\partial x} (Du) - \frac{\eta a'}{a} \frac{\partial}{\partial \eta} (Du) - \frac{\zeta b'}{b} \frac{\partial}{\partial \zeta} (Du) \quad (3.23)$$

$$\frac{\partial^2 u}{\partial y^2} = \frac{\partial}{\partial \eta} \left(\frac{\partial u}{\partial \eta} \frac{\partial \eta}{\partial y} \right) \frac{\partial \eta}{\partial y} = \frac{1}{a^2} \frac{\partial^2 u}{\partial \eta^2} \quad (3.24)$$

$$\frac{\partial^2 u}{\partial z^2} = \frac{\partial}{\partial \zeta} \left(\frac{\partial u}{\partial \zeta} \frac{\partial \zeta}{\partial z} \right) \frac{\partial \zeta}{\partial z} = \frac{1}{b^2} \frac{\partial^2 u}{\partial \zeta^2} \quad (3.25)$$

¹Body forces are neglected. Also local acceleration is neglected due to the fact that analysis is developed under steady state conditions.

where a new operator for viscous term can be defined as,

$$\psi = D^2 + \frac{1}{a^2} \frac{\partial^2}{\partial \eta^2} + \frac{1}{b^2} \frac{\partial^2}{\partial \zeta^2} \quad (3.26)$$

Then replacing the non dimensional forms of coordinates, velocity and pressure onto equation (3.4), (3.5) and (3.6) leads to:

$$\hat{\Gamma} = -\left(\frac{\rho U^2}{\epsilon Re}\right) \left(D + \frac{1}{a} \frac{\partial}{\partial \eta} + \frac{1}{b} \frac{\partial}{\partial \zeta}\right) \hat{p} \quad (3.27)$$

$$\hat{I} = \frac{U}{L} \left(\hat{u} \hat{D} + \frac{\hat{v}}{a} \frac{\partial}{\partial \eta} + \frac{\hat{w}}{b} \frac{\partial}{\partial \zeta}\right) \quad (3.28)$$

$$\hat{\psi} = \frac{1}{L^2} \hat{D}^2 + \frac{1}{(a_o a)^2} \frac{\partial^2}{\partial \eta^2} + \frac{1}{(a_o b)^2} \frac{\partial^2}{\partial \zeta^2} \quad (3.29)$$

and in a more compact form:

$$\hat{\psi} = \frac{1}{(a_o)^2} \left(\epsilon^2 \hat{D}^2 + \frac{1}{a^2} \frac{\partial^2}{\partial \eta^2} + \frac{1}{b^2} \frac{\partial^2}{\partial \zeta^2}\right) \quad (3.30)$$

Therefore, the compact form of the mapped Navier Stokes equation and mass conservation are as follows,

$$\hat{\Gamma} \hat{p} + \mu \hat{\psi} \hat{V} = \rho \hat{I} \hat{V} \quad (3.31)$$

$$\hat{\psi} = \frac{1}{(a_o)^2} \left(\epsilon^2 \hat{D}^2 + \frac{1}{a^2} \frac{\partial^2}{\partial \eta^2} + \frac{1}{b^2} \frac{\partial^2}{\partial \zeta^2}\right) \quad (3.32)$$

Then, expanding the equation for all components leads to the following expressions,

$$\epsilon Re \left(\hat{u} \hat{D} \hat{u} + \hat{v} \frac{\partial \hat{u}}{\partial \eta} + \hat{w} \frac{\partial \hat{u}}{\partial \zeta}\right) = -\hat{D} \hat{p} + \left(\epsilon^2 \hat{D}^2 \hat{u} + \frac{1}{a^2} \frac{\partial^2 \hat{u}}{\partial \eta^2} + \frac{1}{b^2} \frac{\partial^2 \hat{u}}{\partial \zeta^2}\right) \quad (3.33)$$

$$\epsilon \left(\hat{u} \hat{D} \hat{v} + \hat{v} \frac{\partial \hat{v}}{\partial \eta} + \hat{w} \frac{\partial \hat{v}}{\partial \zeta}\right) = -\frac{1}{a \epsilon^2 Re} \frac{\partial \hat{p}}{\partial \eta} + \frac{1}{Re} \left(\epsilon^2 \hat{D}^2 \hat{v} + \frac{1}{a^2} \frac{\partial^2 \hat{v}}{\partial \eta^2} + \frac{1}{b^2} \frac{\partial^2 \hat{v}}{\partial \zeta^2}\right) \quad (3.34)$$

$$\epsilon \left(\hat{u} \hat{D} \hat{w} + \hat{v} \frac{\partial \hat{w}}{\partial \eta} + \hat{w} \frac{\partial \hat{w}}{\partial \zeta}\right) = -\frac{1}{b \epsilon^2 Re} \frac{\partial \hat{p}}{\partial \zeta} + \frac{1}{Re} \left(\epsilon^2 \hat{D}^2 \hat{w} + \frac{1}{a^2} \frac{\partial^2 \hat{w}}{\partial \eta^2} + \frac{1}{b^2} \frac{\partial^2 \hat{w}}{\partial \zeta^2}\right) \quad (3.35)$$

3.2 Solution by Perturbation Approximation

The perturbation analysis for the elliptical varying cross section follows the results presented by Wiley, Pedley and Reily [3] and is developed in detail in what follows.

Lets consider equations (3.4), (3.5) and (3.6) in which perturbation parameter ϵ is several orders of magnitude smaller than the initial values in the series. Then a first group of differential equations can be obtained, which solutions lead to the first approach for the description of the pressure and velocity fields. Thus, the axial component of velocity is determined by the equation,

$$-\frac{\partial \hat{p}}{\partial x} + \frac{1}{a^2} \frac{\partial^2 \hat{u}_o}{\partial \hat{\eta}^2} + \frac{1}{b^2} \frac{\partial^2 \hat{u}_o}{\partial \hat{\zeta}^2} = 0 \quad (3.36)$$

in which pressure is a function of the axial coordinate -x. The result is a Poisson equation for which a solution can be obtained through a mapping process based on the transformations (1.14). The mapping process of the ellipse onto a cylindrical domain enables to consider a(x) and b(x) equal. Then applying the solution process developed in (1.3), the solution for the initial value of the axial velocity component is,

$$\hat{u}_o = \frac{1}{2} \frac{a^2 b^2}{a^2 + b^2} \frac{\partial \hat{p}_o}{\partial x} \left(1 - \eta^2 - \zeta^2 \right) \quad (3.37)$$

or in a non dimensional form:

$$\hat{u}_o = \frac{2}{ab} \left(1 - \eta^2 - \zeta^2 \right) \quad (3.38)$$

where pressure gradient has been expressed as:

$$G_o(x) = -\frac{\partial \hat{p}_o}{\partial x} = -\frac{4(a^2 + b^2)}{a^3 b^3} \quad (3.39)$$

In order to define the initial values of the velocity components v_o and w_o , scalar equations in (3.34) and (3.35) are cross partially derived to eliminate pressure term.

This process requires the following relations to be satisfy.

$$-\frac{1}{\epsilon^2} \frac{\partial^2 \hat{p}_o}{\partial \zeta \partial \eta} + \frac{\partial}{\partial \zeta} \left(\frac{1}{a} \frac{\partial^2 \hat{v}_o}{\partial \eta^2} + \frac{a}{b^2} \frac{\partial^2 \hat{v}_o}{\partial \zeta^2} \right) = 0 \quad (3.40)$$

$$-\frac{1}{\epsilon^2} \frac{\partial^2 \hat{p}_o}{\partial \zeta \partial \eta} + \frac{\partial}{\partial \eta} \left(\frac{b}{a^2} \frac{\partial^2 \hat{w}_o}{\partial \eta^2} + \frac{1}{b} \frac{\partial^2 \hat{w}_o}{\partial \zeta^2} \right) = 0 \quad (3.41)$$

$$\frac{\partial}{\partial \zeta} \left(\frac{1}{a} \frac{\partial^2 \hat{v}_o}{\partial \eta^2} + \frac{a}{b^2} \frac{\partial^2 \hat{v}_o}{\partial \zeta^2} \right) = \frac{\partial}{\partial \eta} \left(\frac{b}{a^2} \frac{\partial^2 \hat{w}_o}{\partial \eta^2} + \frac{1}{b} \frac{\partial^2 \hat{w}_o}{\partial \zeta^2} \right) \quad (3.42)$$

Then by integration process of the equation over the mapped section area expressed in terms of coordinates (η, ζ) , leads the following set of equations,

$$\iint \left(\frac{\partial}{\partial \zeta} \left(\frac{1}{a} \frac{\partial^2 \hat{v}_o}{\partial \eta^2} + \frac{a}{b^2} \frac{\partial^2 \hat{v}_o}{\partial \zeta^2} \right) - \frac{\partial}{\partial \eta} \left(\frac{b}{a^2} \frac{\partial^2 \hat{w}_o}{\partial \eta^2} + \frac{1}{b} \frac{\partial^2 \hat{w}_o}{\partial \zeta^2} \right) \right) d\eta d\zeta = 0 \quad (3.43)$$

$$\int \left(\frac{1}{a} \frac{\partial^2 \hat{v}_o}{\partial \eta^2} + \frac{a}{b^2} \frac{\partial^2 \hat{v}_o}{\partial \zeta^2} \right) d\eta = \int \left(\frac{b}{a^2} \frac{\partial^2 \hat{w}_o}{\partial \eta^2} + \frac{1}{b} \frac{\partial^2 \hat{w}_o}{\partial \zeta^2} \right) d\zeta = -A(\eta, \zeta) \quad (3.44)$$

The integration process gives rise to an arbitrary function $A(\eta, \zeta)$ that must be evaluated according to boundary conditions. Then expressing the equations in differential form leads to,

$$\left(\frac{1}{a} \frac{\partial^2 \hat{v}_o}{\partial \eta^2} + \frac{a}{b^2} \frac{\partial^2 \hat{v}_o}{\partial \zeta^2} \right) = -\frac{\partial A(\eta, \zeta)}{\partial \eta} \quad (3.45)$$

$$\left(\frac{b}{a^2} \frac{\partial^2 \hat{w}_o}{\partial \eta^2} + \frac{1}{b} \frac{\partial^2 \hat{w}_o}{\partial \zeta^2} \right) = -\frac{\partial A(\eta, \zeta)}{\partial \zeta} \quad (3.46)$$

Considering that derivatives of the arbitrary function A with respect to coordinate variables are constant, two Poisson equations are obtained. Therefore a mapping process onto a cylindrical coordinates as in (1.14) can again be applied as follows.

$$v_o = -\frac{1}{4} \frac{\partial A}{\partial \eta} (1 - \eta^2 - \zeta^2) \quad (3.47)$$

$$w_o = -\frac{1}{4} \frac{\partial A}{\partial \zeta} (1 - \eta^2 - \zeta^2) \quad (3.48)$$

Then evaluating continuity equation by mean of velocity components in expressions

(3.47) and (3.48) leads to,

$$\frac{1}{a} \frac{\partial \hat{v}_o}{\partial \eta} - \frac{1}{b} \frac{\partial \hat{w}_o}{\partial \zeta} = \frac{2(ab)'}{a^2 b^2} (1 - \eta^2 - \zeta^2) - \frac{4}{ab} \left(\frac{a'}{a} \eta^2 + \frac{b'}{b} \zeta^2 \right) \quad (3.49)$$

$$\frac{1}{2a} \frac{\partial A}{\partial \eta} - \frac{1}{2b} \frac{\partial A}{\partial \zeta} = \frac{2(ab)'}{a^2 b^2} (1 - \eta^2 - \zeta^2) - \frac{4}{ab} \left(\frac{a'}{a} \eta^2 + \frac{b'}{b} \zeta^2 \right) \quad (3.50)$$

The relation between η, ζ is determined by,

$$\eta^2 + \zeta^2 = 1 \quad (3.51)$$

in which the range of variables is (0,1). Hence the arbitrary functions are determined

as,

$$\frac{\partial A}{\partial \eta} = -\frac{8}{ab} (a' \eta) \quad (3.52)$$

$$\frac{\partial A}{\partial \zeta} = \frac{8}{ab} (b' \zeta)$$

and finally the velocity field for the initial values is entirely defined.

$$v_0 = \frac{2a'\eta}{ab} (1 - \eta^2 - \zeta^2) \quad (3.53)$$

$$w_0 = \frac{2b'\zeta}{ab} (1 - \eta^2 - \zeta^2) \quad (3.54)$$

After the initial values for the velocity components are known, the first perturbation can be determined. Considering the scalar component in the x- direction of equation

(3.33), the first perturbation of axial velocity u_1 and pressure p_1 can be determined.

Writing the equation in terms of the known initial values $\hat{u}_o, \hat{v}_o, \hat{w}_o$ and the ones corresponding to the first perturbation, the Navier Stokes equation takes the following form.

$$\epsilon Re \left(\hat{u}_o \hat{D} \hat{u}_o + \hat{v}_o \frac{\partial \hat{u}_o}{\partial \eta} + \hat{w}_o \frac{\partial \hat{u}_o}{\partial \zeta} \right) = -\epsilon \frac{\partial \hat{p}_1}{\partial x} + \epsilon \left(\frac{1}{a^2} \frac{\partial^2 \hat{u}_1}{\partial \eta^2} + \frac{1}{b^2} \frac{\partial^2 \hat{u}_1}{\partial \zeta^2} \right) \quad (3.55)$$

Considering each term of the convective acceleration individually for clarity and evaluating (3.53) and (3.54), the form of the Navier Stokes equation is:

$$\hat{u}_o \hat{D} \hat{u} = \frac{2(1-\eta^2-\zeta^2)}{(ab)} \left(-\frac{2(ab)'(1-\eta^2-\zeta^2)}{(ab)^2} + \frac{2a'\eta^2}{a} + \frac{2b'\zeta^2}{b} \right) \quad (3.56)$$

$$\hat{v}_o \frac{\partial \hat{u}_o}{\partial \eta} = -\frac{2a'(1-\eta^2-\zeta^2)}{(ab)} \left(\frac{4\eta^2}{ab} \right) \quad (3.57)$$

$$\hat{w}_o \frac{\partial \hat{u}_o}{\partial \zeta} = -\frac{2b'(1-\eta^2-\zeta^2)}{(ab)} \left(\frac{4\zeta^2}{ab} \right) \quad (3.58)$$

$$\left(\frac{1}{a^2} \frac{\partial^2 \hat{u}_1}{\partial \eta^2} + \frac{1}{b^2} \frac{\partial^2 \hat{u}_1}{\partial \zeta^2} \right) = -\frac{\partial \hat{p}_1}{\partial x} - Re \frac{4(ab)'(1-\eta^2-\zeta^2)^2}{(ab)^3} \quad (3.59)$$

where pressure gradient for the first perturbation is also a function of the x- coordinate. Solution of equation (3.59) is developed applying a new mapping process onto a cylindrical coordinates system. The complete procedure towards the solution is presented in what follows:

First new variables are defined in order to simplify expressions in equation (3.59).

$$G_1 = -\frac{\partial \hat{p}_1}{\partial x} K = \frac{4(ab)'}{(ab)^3} \quad (3.60)$$

then equation (3.58) is expressed in terms of cylindrical coordinates as follows.

$$\frac{1}{r} \frac{\partial}{\partial r} \left(r \frac{\partial \hat{u}_1}{\partial r} \right) = G_1 - KRe(1-r^2)^2 \quad (3.61)$$

Integration of equation (3.60) is straightforward and the boundary condition of zero velocity at the tube wall persists. Thus, solution of the first perturbation for velocity is:

$$\hat{u}_1 = \frac{G_1}{4} (R^2 - r^2) - KRe \left[\frac{R^2 - r^2}{4} - \frac{R^4 - r^4}{8} + \frac{R^6 - r^6}{36} \right] \quad (3.62)$$

Flow Rate

Considering the η, ζ domain in which $0 < R < 1$, the integration process to determine an expression for flow is straightforward.

$$q_1 = \int_0^1 \left[\frac{G_1}{4} (R^2 - r^2) - KRe \left[\frac{R^2 - r^2}{4} - \frac{R^4 - r^4}{8} + \frac{R^6 - r^6}{36} \right] \right] 2\pi r dr \quad (3.63)$$

Considering $q_1 = 0$, which means that no flow is due to the perturbed velocity, the following result is obtained,

$$q_1 = 0 = \left[\frac{G_1}{16} + \frac{KRe}{32} \right] \quad (3.64)$$

Pressure Gradient

From equation (3.65) the first perturbation for pressure gradient is determined as,

$$G_1(x) = -\frac{2(ab)'Re}{(a^3b^3)} \quad (3.65)$$

which is a function of cross section area variation along the tube length and independent of its shape.

Then considering equations (3.39) and (3.64) the final form of the pressure gradient including the perturbation can be determined as follows:

$$\frac{\partial \hat{p}}{\partial x} = \frac{4(a^2 + b^2)}{a^3b^3} - \left(\frac{2(ab)'Re}{(a^3b^3)} \right) \quad (3.66)$$

where \hat{p} is defined by $\hat{p}_o + \epsilon \hat{p}_1$.

Equation (3.65) represents the non dimensional form of pressure gradient for a varying cross section corrected by perturbation.

Axial Velocity

Considering equation (3.38) and (3.61) the first perturbation that corresponds to the axial component of velocity can be expressed in the scaled coordinate system η, ζ .

$$u_1 = \frac{G_1}{4}(1-r^2) + KRe(1-r^2) \left[\frac{1}{4} - \frac{1+r^2}{8} + \frac{(1+r^2+r^4)}{36} \right] \quad (3.67)$$

$$u_1 = \frac{(1-r^2)}{4} \left(G_1 + KRe \left[1 - \frac{1+r^2}{2} - \frac{(1+r^2+r^4)}{9} \right] \right) \quad (3.68)$$

$$u_1 = \frac{(1-\eta^2-\zeta^2)}{2} \frac{Re(ab)'}{a^3 b^3} \left(1+2 \left[1 - \frac{1+(\eta^2+\zeta^2)}{2} - \frac{(1+(\eta^2+\zeta^2)+(\eta^2+\zeta^2)^2)}{9} \right] \right) \quad (3.69)$$

and the final expression for the axial velocity component is,

$$\hat{u} = \frac{2}{ab} (1-\eta^2-\zeta^2) + \epsilon \left(\frac{(1-\eta^2-\zeta^2)}{2} \frac{Re(ab)'}{a^3 b^3} \left(1+2 \left[1 - \frac{1+(\eta^2+\zeta^2)}{2} - \frac{(1+(\eta^2+\zeta^2)+(\eta^2+\zeta^2)^2)}{9} \right] \right) \right) \quad (3.70)$$

which constitutes the solution by a first order perturbation. It is important to establish the range for which *lubrication approximation* and *asymptotic perturbation* are valid. This will depend upon geometry of cross section as well as changes in steepness along the tube length.

Chapter 4

Implementation of Numerical Solutions on Practical Cases

Theoretical aspects of analytic and numerical methods that enable solution of laminar flow across tubes of arbitrary varying cross section, have been explored so far. In this chapter numerical solutions are implemented for some specific cases. To establish the range of validity of the methods, results are compared against data obtained from a commercial CFD software.

Numerical solutions for constant cross section have been discussed in detail in chapter 2, verifying that unit velocity distributions are in accordance to analytic results. Numerical experiments that are developed in what follows, are intended to address the capability of numerical methods to predict pressure distribution for varying cross sections. Elliptical cross sections are employed due to the fact that some analytic results are available for comparison purposes.

4.1 Design of Numerical Experiments Procedure

Numerical experiments developed in what follows apply *numerical lubrication, numerical perturbations alternative perturbation* and perturbation with *convective acceleration correction*, to two elliptical sections with different aspect ratio defined by the quotient between semi-axis (a) and total length L. Furthermore, an square section with the same aspect ratio of the ellipsis and also linear variation of cross section, is tested as a more general case.

Several flow rates scaled by velocity are tested, which values are based on a reference flow rate corresponding to a mean velocity of 1 (mm/sec) . To avoid unstable behaviors, all flow rates impose Reynolds numbers below 250.

Then, pressure gradients are calculated applying equation (2.21), and pressure distribution along the tube length is calculated by numerical integration using trapezoidal rule as follows.

$$p_{x+\Delta x} = p_x + \left(\frac{\Delta p_{x+\Delta x}}{\Delta x} + \frac{\Delta p_x}{\Delta x} \right) \frac{\Delta x}{2} \quad (4.1)$$

Uncertainties are determined comparing results from numerical methods, against data generated using a commercial CFD *computational fluid dynamics* software. Considering that CFD software enables Navier Stokes solution in three-dimensional space, results are considered more accurate than those obtained with the numerical procedures.

Experiment Definition

Two tests performed on elliptical cross section for different aspect ratios are presented and eccentricity of 0.5. Details of elliptical tube and experimental parameters

are shown in figure and table 4.1 respectively.

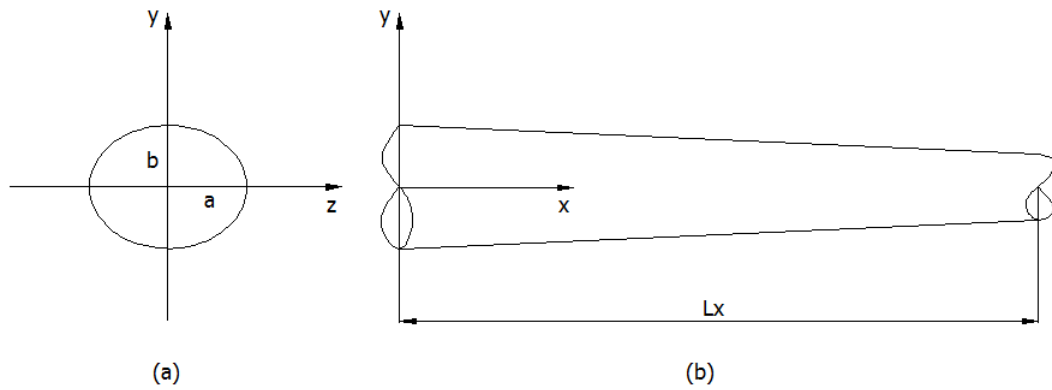


Figure 4.1: Elliptical section with eccentricity b/a

Variable	Symbol	Unit	Value
Dynamic Viscosity	μ	[Pa.sec]	1.002×10^{-3}
Density	ρ	[Kg/m ³]	998
Major Axis	a	[mm]	10
Eccentricity	b/a	[mm/mm]	0.50
Section Variation	m	[mm/mm]	1/200 2/200
Reference Flow Rate	q_{ref}	[m ³ /sec]	1.5708×10^{-7}
Flow Rate Range	q_i	$q_i = (1, 3, 5, 7, 9, 11, 13) \cdot q_{ref}$	

Table 4.1: Flow properties and geometry description

4.2 Results of Numerical Experiments

4.2.1 Influence of Aspect Ratio on Pressure Distribution

Pressure distribution along the tube and the effect of aspect ratio (1/200) and (2/200) is presented for $q_i = 5q_{ref}$, which approximately represents the center of the flow rate span analyzed for all cases.

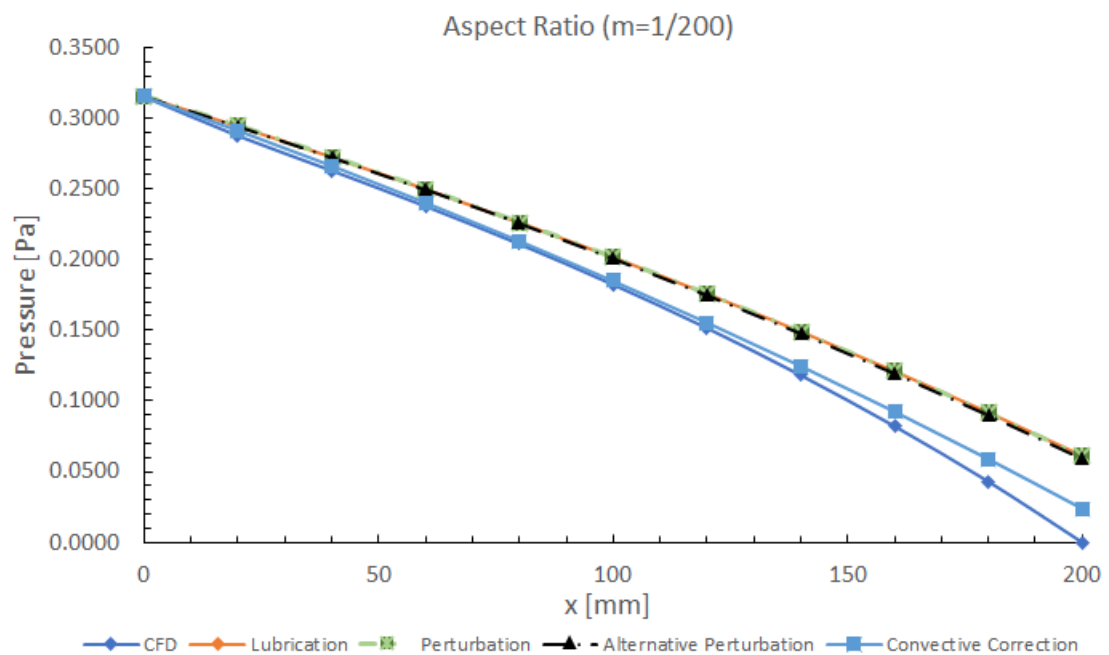


Figure 4.2: Pressure Distribution (m=2/200)

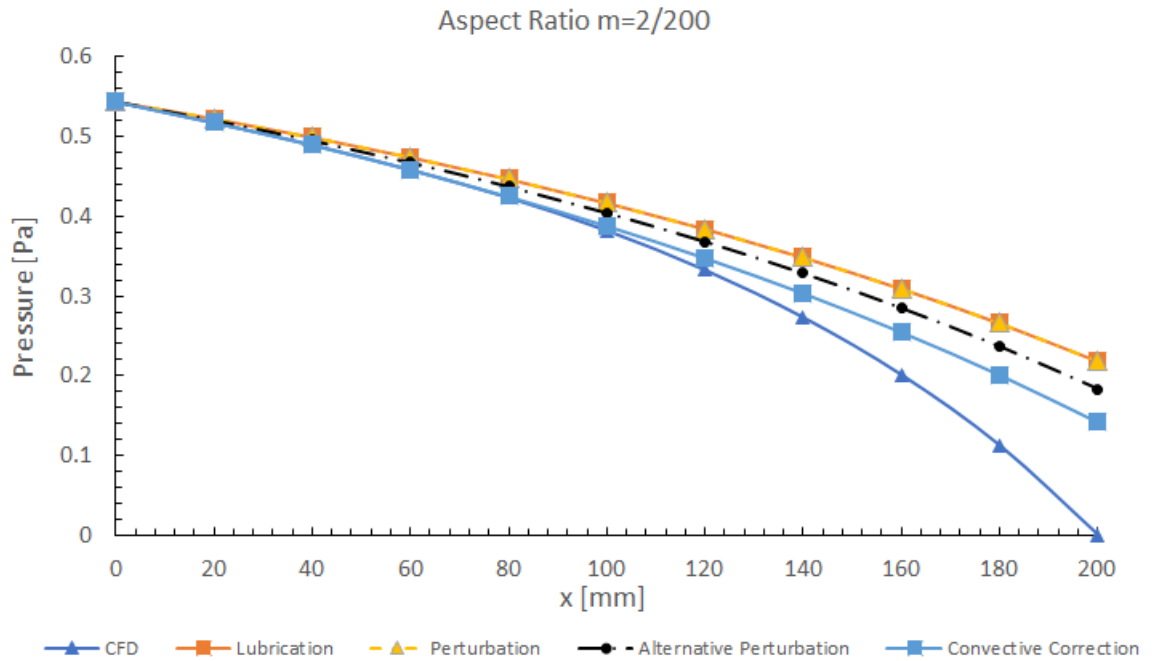


Figure 4.3: Pressure Distribution ($m=2/200$)

Results shows that prediction of *pressure distribution* is more accurate for smooth variations of sections, which implies smaller values for local pressure gradients.

Deviation of pressure values from the CFD results, is caused by the progressive effect that convective acceleration has on the velocity field. This is probably the reason why convective correction exhibits better approach to CFD than the other numerical methods. To demonstrate this observation, pressure distributions for extreme values of flow rates are presented for both aspect ratios.

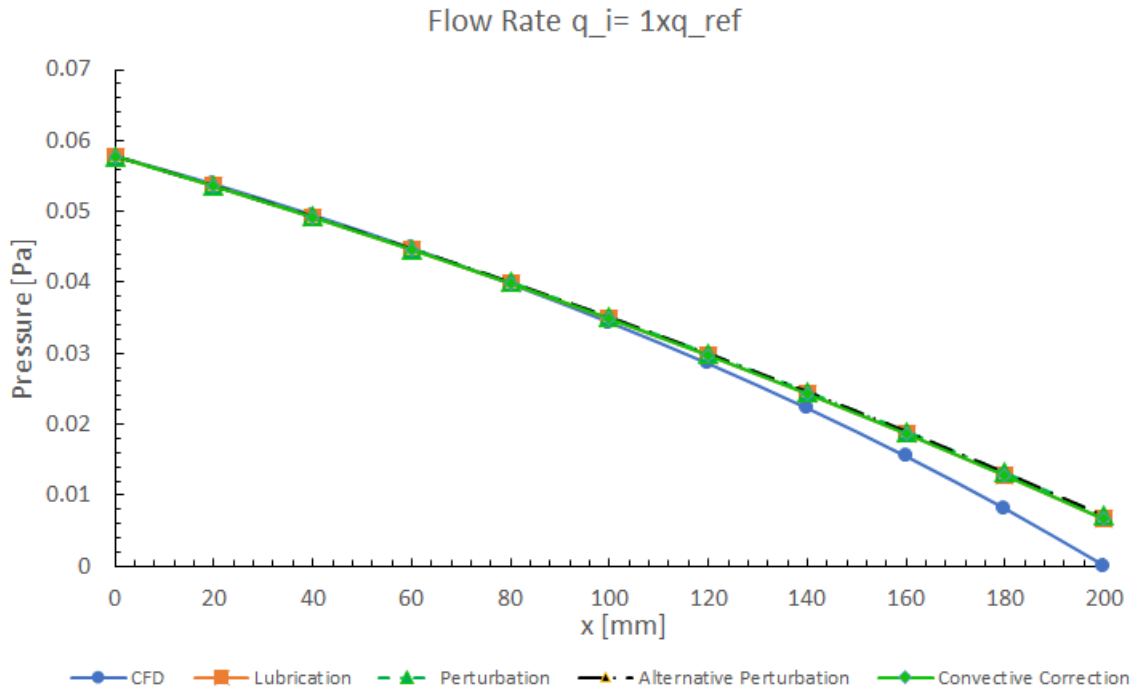


Figure 4.4: Pressure Distribution: Flow rate $q_1, ellipse (b/a=1/2, m=1/200)$

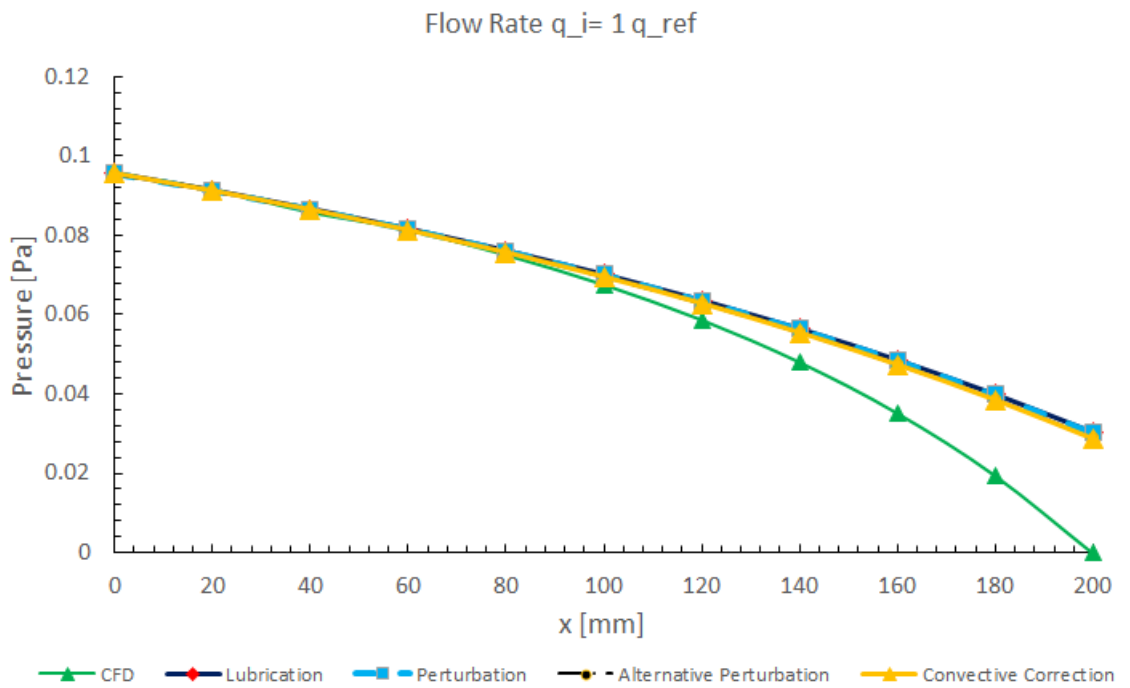


Figure 4.5: Pressure Distribution: Flow rate $q_{13}, ellipse (b/a=1/2, m=1/200)$

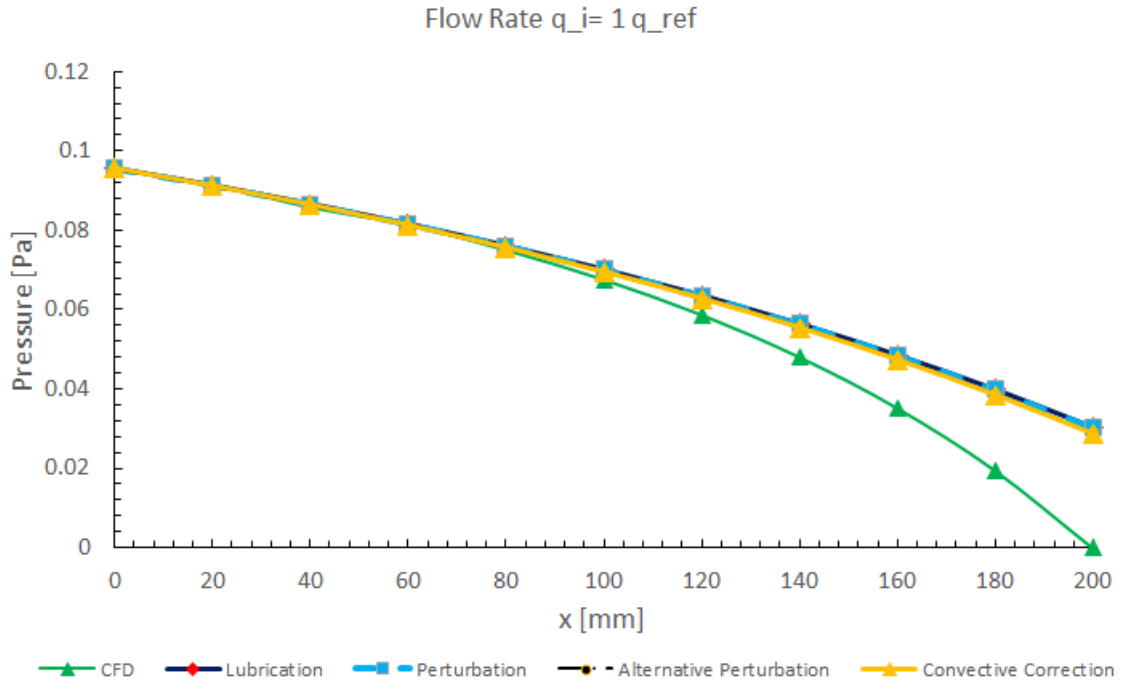


Figure 4.6: Pressure Distribution: Flow rate q_1 , ellipse ($b/a=1/2, m=2/200$)

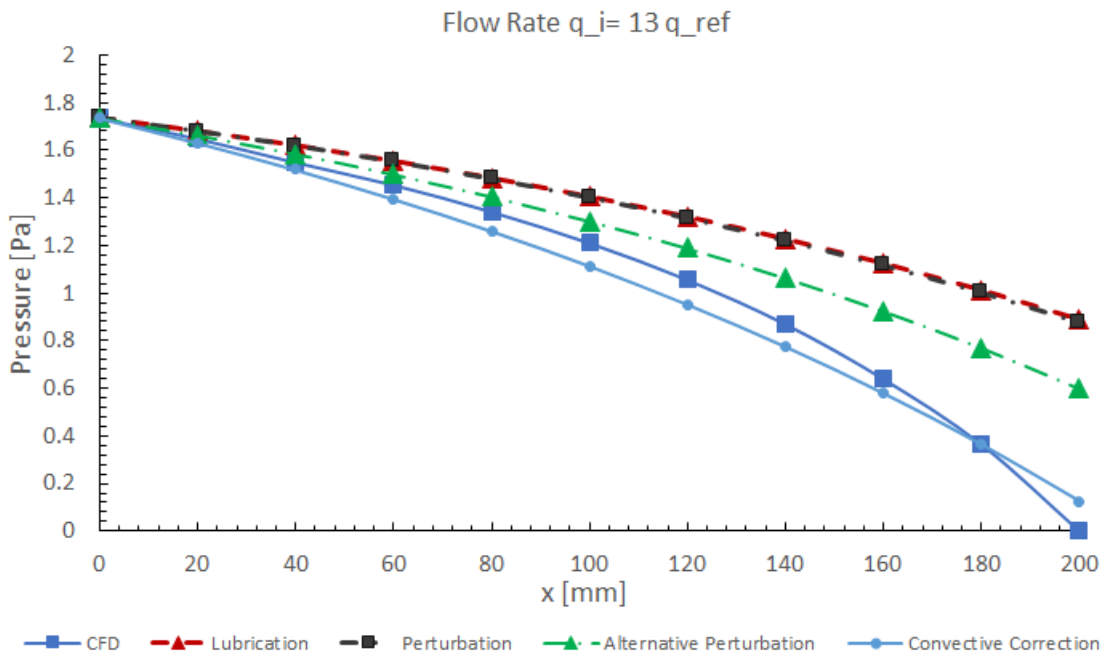


Figure 4.7: Pressure Distribution: Flow rate q_{13} , ellipse ($b/a=1/2, m=2/200$)

4.2.2 Uncertainty Analysis for Ellipse

To address uncertainty in *pressure distribution* along tube length, relative errors are calculated for each ellipse and numerical method. Results are presented in what follows.

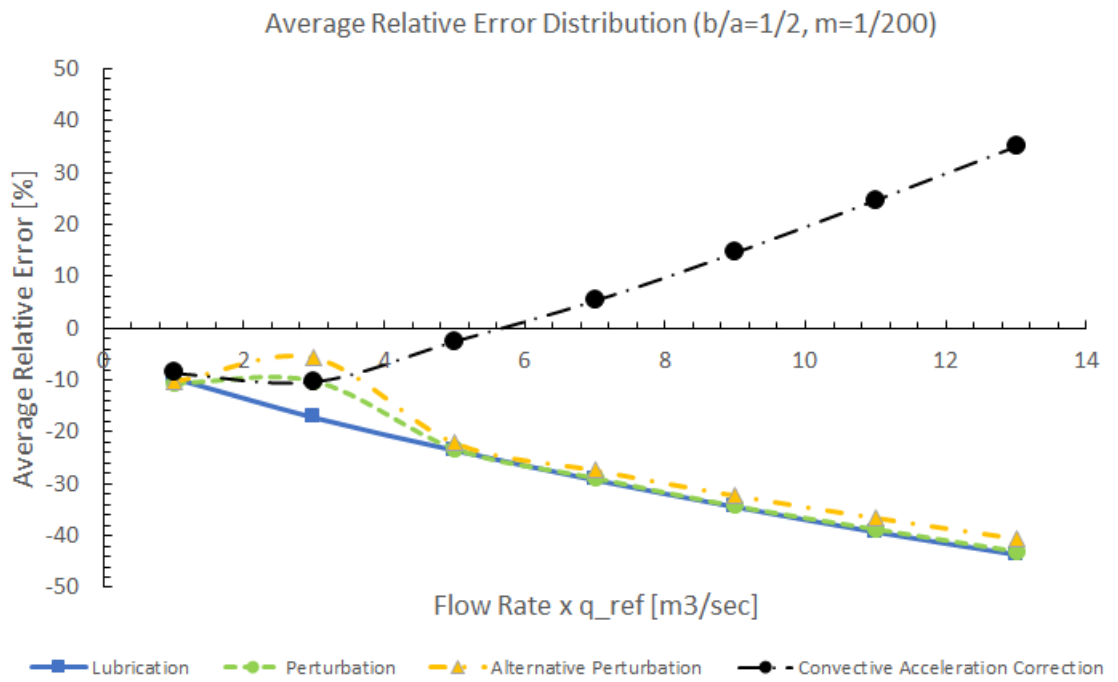


Figure 4.8: Pressure Relative Error ($b/a=1/2, m=1/200$)

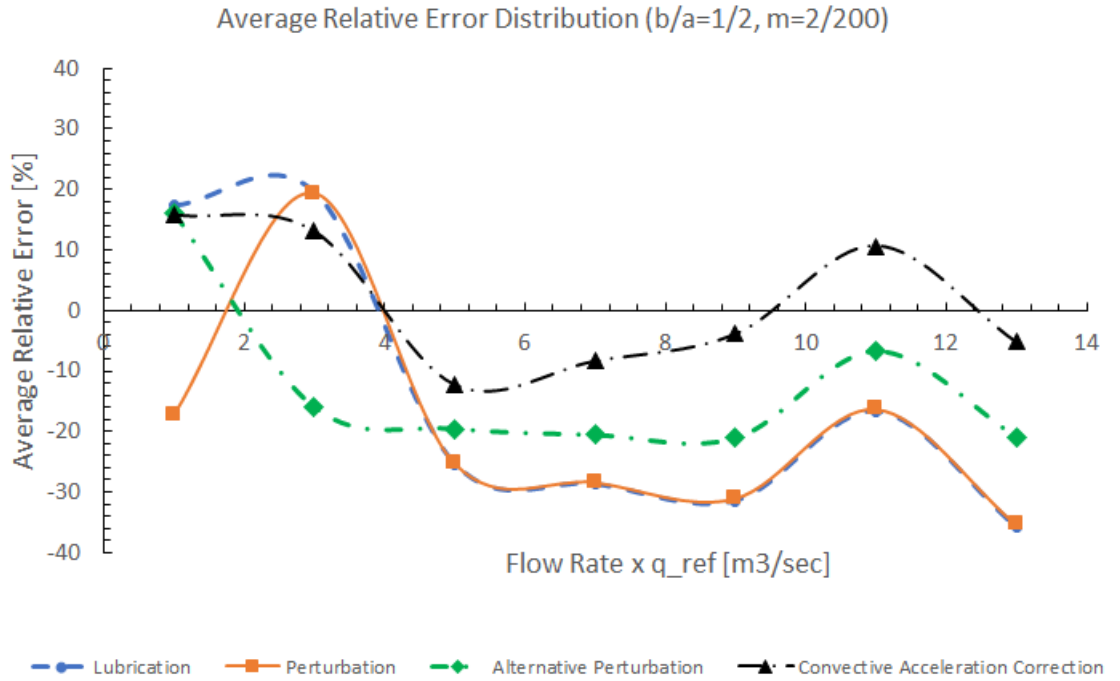


Figure 4.9: Pressure Relative Error ($b/a=1/2, m=2/200$)

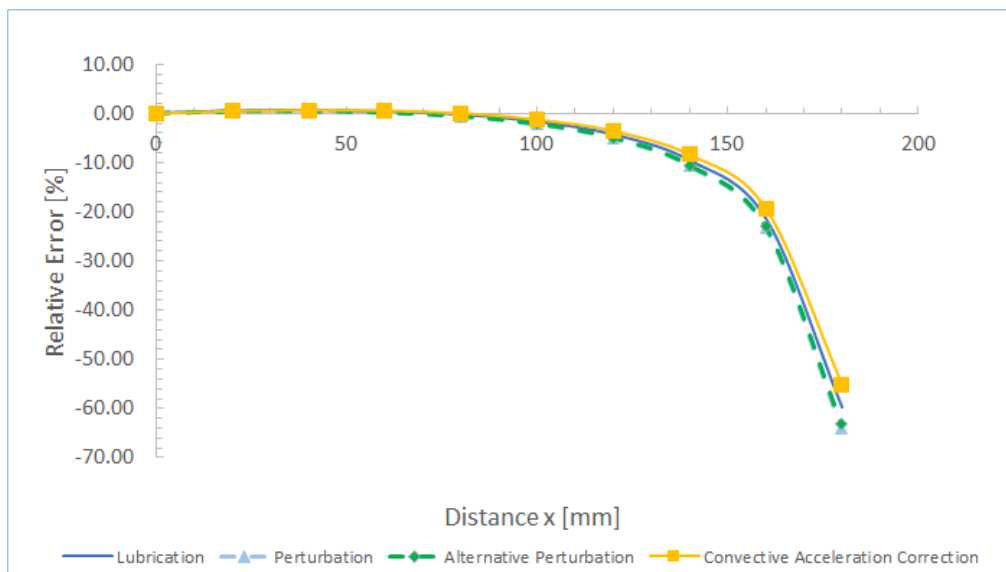


Figure 4.10: Pressure Relative Error Flow Rate q_1 ($b/a=1/2, m=1/200$)

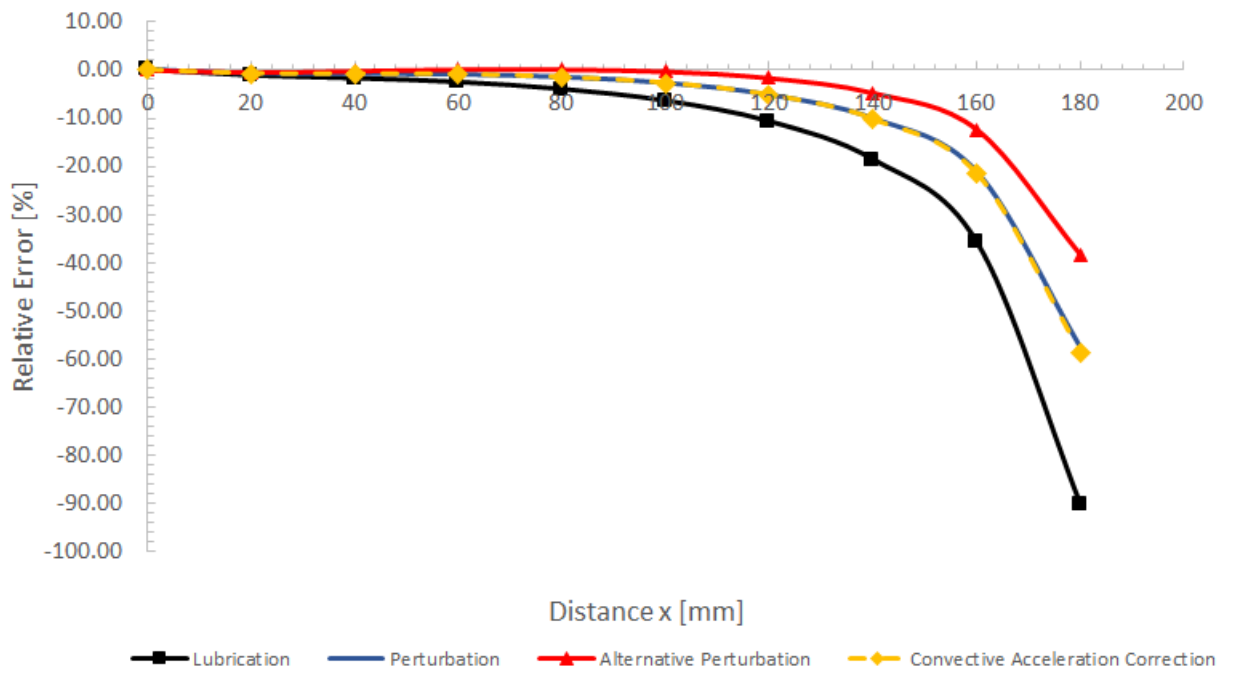


Figure 4.11: Pressure Relative Error Flow Rate q3 ($b/a=1/2, m=1/200$)

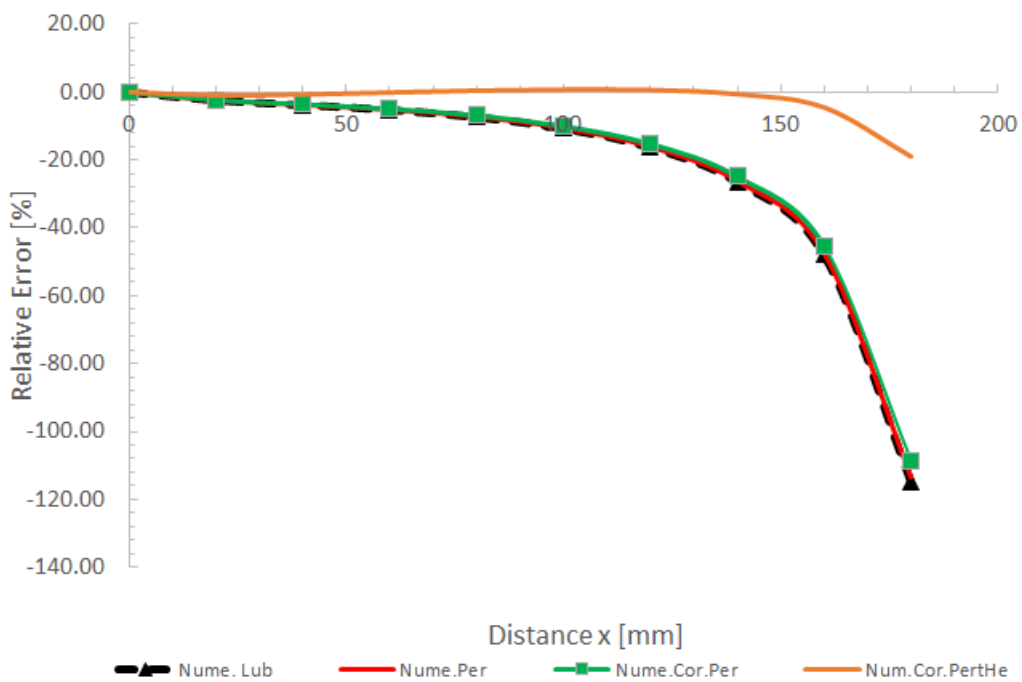


Figure 4.12: Pressure Relative Error Flow Rate q5 ($b/a=1/2, m=1/200$)

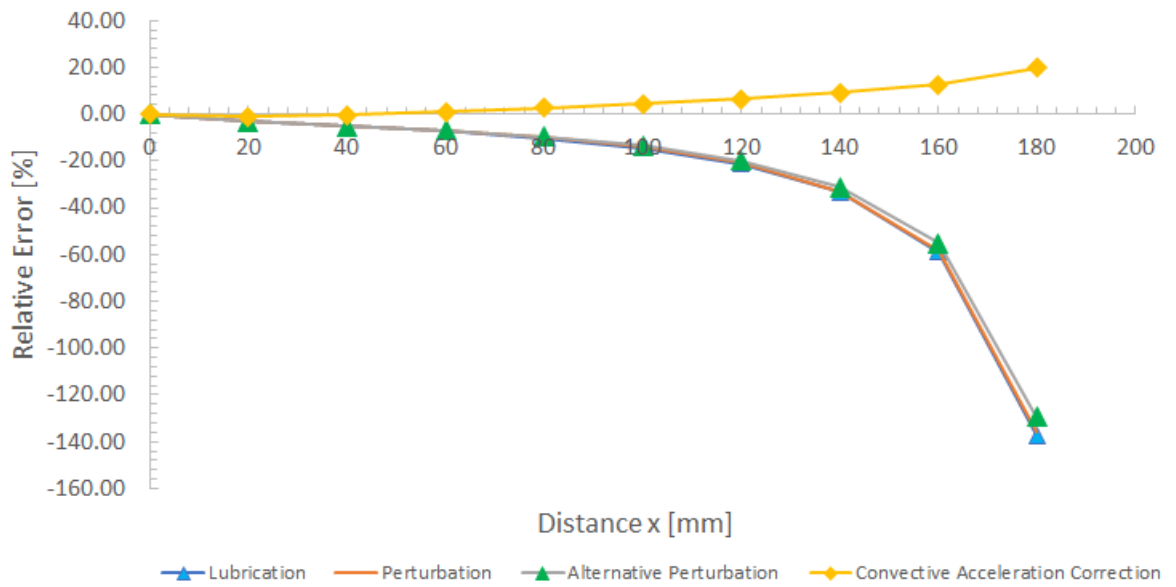


Figure 4.13: Pressure Relative Error Flow Rate q7 ($b/a=1/2, m=1/200$)

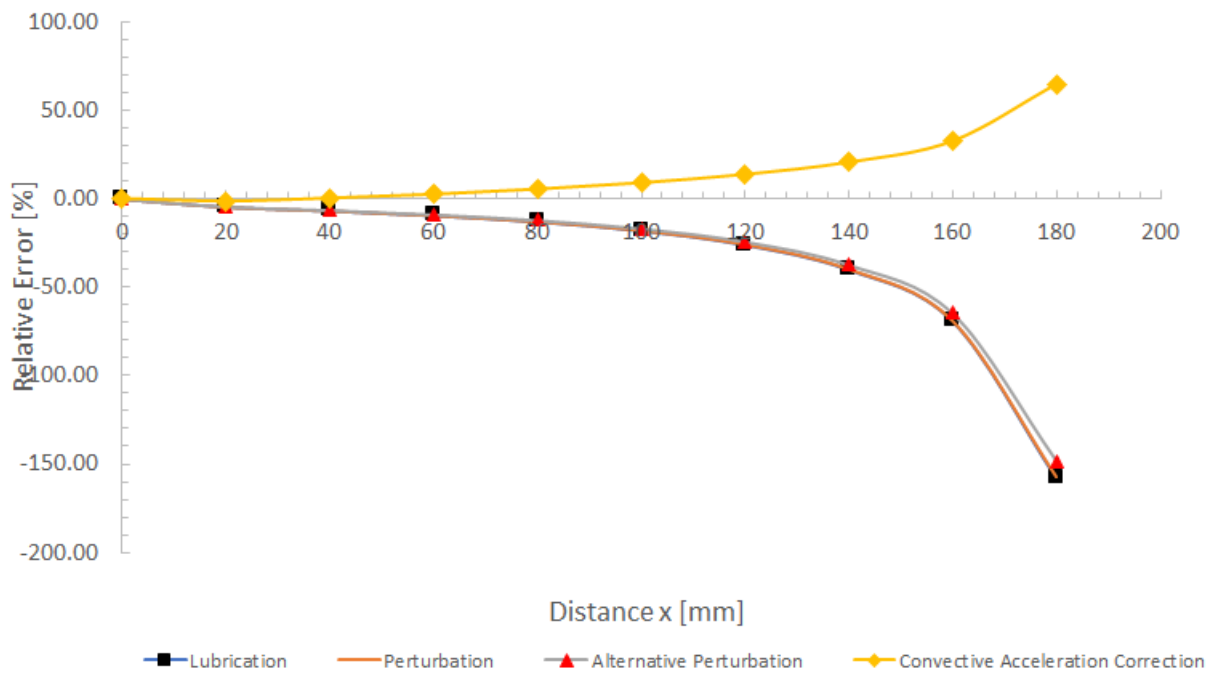


Figure 4.14: Pressure Relative Error Flow Rate q9 ($b/a=1/2, m=1/200$)

Analysis of a Rectangular Section

As an extension of previous methods, a rectangular cross section is studied for the maximum flow rate. Results are presented in what follows,

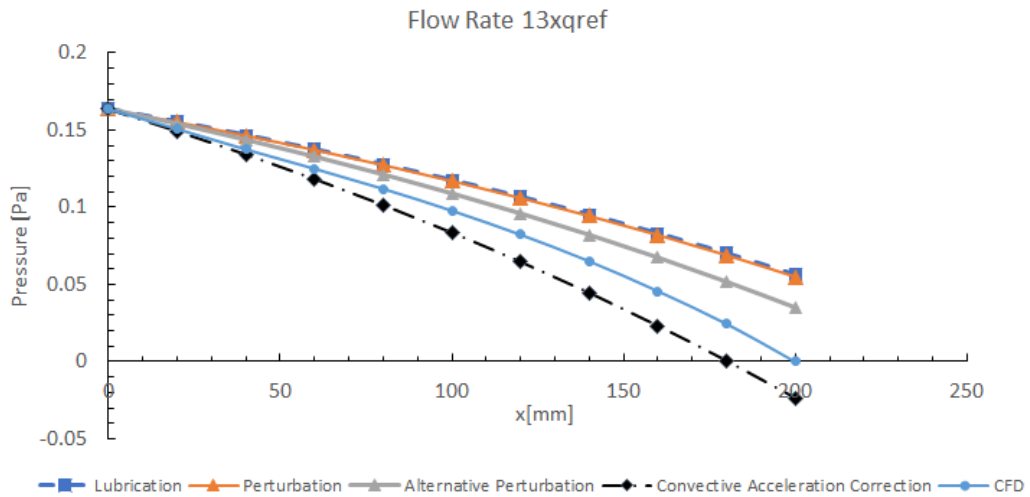


Figure 4.15: Pressure Distribution Rectangle ($b/a=1/2, m=2/200$)

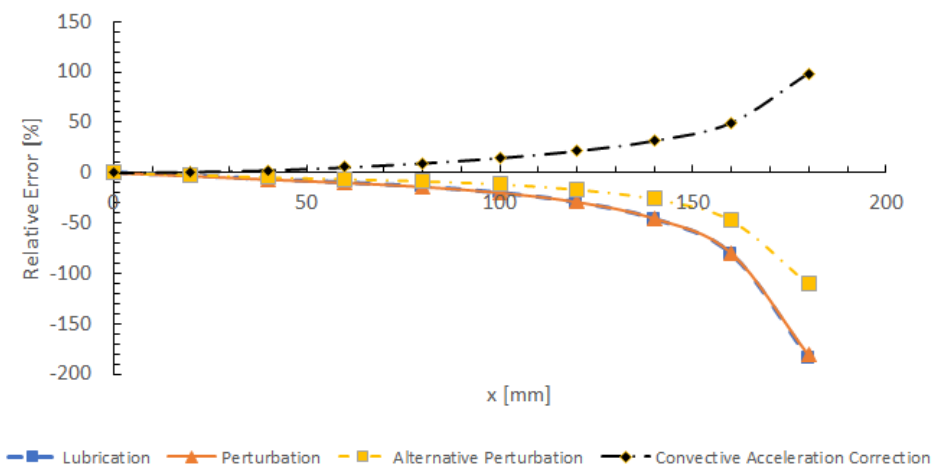


Figure 4.16: Relative Error Rectangle Flow Rate q13 ($b/a=1/2, m=1/200$)

In this example, Reynolds number is at a higher limit of 200. At this flow regime, all the methods developed for pressure estimation exhibit large error values, and convective acceleration correction has the smaller relative error.

Response of the different analysis methods for pressure estimation follow the same tendency. Results show that perturbation methods including the convective acceleration correction, exhibit less uncertainty with respect to the CFD solution used as

reference. For the case of the large flow rates, all perturbations exhibit higher relative errors. Moreover, relative errors have the smaller values for flow rates between $5q_{ref}$ and $7q_{ref}$, which correspond to Reynolds number between $50 < Re < 150$.

Chapter 5

Conclusions

Analytic and numerical procedures that enable to obtain velocity distributions and pressure gradients, for Newtonian viscous flows across arbitrary varying cross section have been developed. Solutions by numerical lubrication method leads to the same results as its analytic counterpart. The use of non dimensional models combined with finite element procedures and appropriate scaling factors, proved to be effective means to predict velocity distributions and pressure gradients for a broader range of arbitrary cross sections. Furthermore, estimation of Poiseuille numbers extracted from numerical solutions in a non dimensional form, enables to explore Fanning friction factors for complex shapes in laminar regime, which on the other hand, is the first step to explore turbulent friction factors.

Beyond the classical methods, two perturbation procedures have been explored. An alternative perturbation applied directly to velocity in viscous and axial convective acceleration terms, proved to be effective in estimation of pressure gradients for sections with sharper aspect ratios. Perturbation parameter following definition of non dimensional velocity and flow rate was derived in terms of characteristic length, area

derivative and area cross section. This regular perturbation method represents a generalization of classical procedure extensively employed in Fluid Mechanics, which combined with numerical method enables solution of a broader range of cases.

Finally, the use of perturbation approximation applied to the entire convective acceleration term in Navier Stokes equation has been tested. In this case, a new perturbation parameter based on aspect ratio and Reynolds number was defined and added to the regular perturbation previously defined. Pressure gradients calculated by means of this correction, exhibited less average relative error than any other tested method when results were compared to CFD solutions. However, estimations obtained by this method require an in deep exploration to address a broader range of applicability.

In all methods explored, results demonstrated to be highly sensitive to definition of characteristic length. Parameters recommended in literature, like hydraulic diameter, square root of area cross section or perimeter, may not be the best option as scaling factor for non dimensional solutions. Instead, radius for circular cases, semi axis for ellipsis and rectangles or polar radius functions employed to generate the closed shape , proven to be appropriate parameters leading to more accurate solutions.

Bibliography

- [1] F. White, *Viscous Flow*, McGraw-Hill Inc, 1991.
- [2] M. Akbari a, D. Sinton b, M. Bahrami, "*Viscous flow in variable cross-section microchannels of arbitrary shapes*," *Journal of Heat and Mass Transfer*, May 2011.
- [3] R.Wild, T.J. Pedley, D.S. Riley, "*Viscous flow in collapsible tubes of slowly varying elliptical cross-section*," *Journal of Fluid Mechanics* vol.81, part 2,pp.273-294,1977
- [4] Y.S.Muzychka,M.M.Yovanovich, "*Pressure Drop in Laminar Developing Flow in Noncircular Ducts:A Scaling and Modeling Approach*," *Journal of Fluids Engineering*, vol 131, 2009
- [5] William M. Deen, *Analysis of Transport Phenomena*,Second Edition, Oxford University Press, 2012
- [6] Computer codes are available upon request.

Vitae

Edgardo Fernández born in Buenos Aires, Argentina on June 20th 1976. He attended to Army Polytechnic School in Ecuador graduating in Mechanical Engineering in 2002(Six years program). He has been involved in the steel industry working as researcher and consultant for companies in Argentina, Brasil, Colombia and Ecuador. He is co-founder of a company dedicated to solution of industrial problems by numerical simulations methods. He is also instructor in the course of Introduction to Fluid Mechanics at Army Polytechnic School in Quito Ecuador. He began the master science program in the fall of 2014.